Patient-Robot-Therapist Collaboration Using Resistive Impedance Controlled Tele-robotic Systems Subjected to Time Delays

Mojtaba Sharifi [a,b]
[a] Department of Mechanical Engineering, Sharif University of Technology
Azadi St., P.O. Box: 11155-9567, Tehran, Iran
[b] Department of Electrical and Computer Engineering, University of Alberta, Edmonton, Alberta, T6G 1H9 Canada
sharifi3@ualberta.ca

Hassan Salarieh[1]
Department of Mechanical Engineering, Sharif University of Technology
Azadi St., P.O. Box: 11155-9567, Tehran, Iran
salarieh@sharif.edu

Saeed Behzadipour
Department of Mechanical Engineering, Sharif University of Technology
Azadi St., P.O. Box: 11155-9567, Tehran, Iran
behzadipour@sharif.edu

Mahdi Tavakoli
Department of Electrical and Computer Engineering, University of Alberta, Edmonton, Alberta, T6G 1H9 Canada
mahdi.tavakoli@ualberta.ca

ABSTRACT

In this paper, an approach to physical collaboration between a patient and a therapist is proposed using a bilateral impedance control strategy developed for delayed tele-robotic systems. The patient performs a tele-rehabilitation task in a resistive virtual environment with the help of online assistive forces from the therapist being provided through teleoperation. Using this strategy, the patient's involuntary hand tremors can be filtered out and the effort of severely impaired patients can be amplified in order to facilitate their early engagement in physical tasks. The response of the first desired impedance model is

[1] Corresponding author.

tracked by the master robot (interacting with the patient), and the master trajectory plus a deviation as the response of the second impedance model is tracked by the slave robot (interacting with the therapist). Note that the first impedance model is a virtual mass-damper-spring system that has a response trajectory to the combination of patient and therapist forces. Similarly, the second impedance model is a virtual mass-damper-spring system that generates the desired slave-master deviation trajectory as its response to the therapist force. Transmitted signals through the communication channels are subjected to time delays, which exist in home-based rehabilitation (i.e., tele-rehabilitation). Tracking of the impedance models responses in the presence of modeling uncertainties is achieved by employing a nonlinear bilateral adaptive controller and proven using a Lyapunov analysis. The stability of delayed teleoperation system is also proven using the absolute stability criterion. The proposed control method is experimentally evaluated for patient-therapist collaboration in resistive/assistive tasks. In these experiments, a healthy human operator simulates a post-stroke patient behavior during the interaction with the master robot.

1. INTRODUCTION

Stroke, multiple sclerosis, cerebral palsy, and Parkinson's disease are some of age-related disorders that bring different disabilities for the patient. Among them, stroke is a main cause of serious long-term disabilities among adults and the second leading cause of death worldwide [1]. There are 6.6 million stroke survivors only in the United States and their treatment and care costs are over $33 billion per year [2].

In order to decrease these costs and provide consistent and reproducible rehabilitation services with less fatigue for the therapist, robotic systems have been employed [3-5]. Some robotic rehabilitation systems have been developed including only one robot for interaction with the patient [6-9]. However, a second robot is required to interact with the therapist to perform various movements and functional

therapies with a collaborative interaction between the patient and therapist employing a bilateral tele-robotic system. This is useful for the remote home-based therapy of patients instead of hospital-based ones.

Note that the rehabilitation therapy using a single-robot and virtual reality (VR) involves the visualization of an environment and providing the haptic force feedback during interaction of the patient with virtual objects [10, 11]. However, tele-rehabilitation systems enable the therapist to share the required physical experiences with remote patients in different tasks during home-based therapy scenarios [10]. The collaborative tele-rehabilitation is an effective way for stimulating post-stroke patients to be more compliant, and the experience-sharing can enhance their motivation and engagement in the therapy process [12]. Realized exercises by these teleoperation systems have resulted in considerable improvements to the patients' motor control [12]. Moreover, employing a tele-robotic system between geographically separated users (patient and therapist) enables them to display their force-position actions to each other through a connected network [11].

Accordingly, robotic tele-rehabilitation has been suggested in [10-17] and unilateral [13, 14] and bilateral [11, 18] control strategies have been used through a shared virtual environment (SVE). In these strategies [11, 13, 14], the positions of two robots have been employed to obtain and reflect haptic feedback from the SVE to the patient and the therapist via their respective robots. Interaction force measurement has been used in [15, 18] to better reflect the force. A trilateral architecture has also been proposed in [17, 19] for mirror therapy of patients, and different multilateral strategies

have been studied in [20] for training some trainees by the therapist during rehabilitation of a patient.

In the past two decades, some control strategies have been presented for linear single-DOF tele-robotic systems [21-23]. In order to perform complex therapy exercises, however, nonlinear multi-DOF systems are needed. With the purpose of position synchronization between the nonlinear master and slave robots, some adaptive bilateral control strategies [24-27] have been suggested in recent years. For simultaneous position tracking and force reflection, nonlinear adaptive position-force control methods [28-30] have been proposed. Instead of position and force control methods, the impedance control strategy [31-33] can realize interactive rehabilitation tasks by providing an adjustable flexibility between the patient and robot [7, 34]. In this strategy, the operator (patient) perceives the adjusted virtual impedance model as the haptic sense during the physical interaction. The impedance control has also been used for linear one-DOF bilateral tele-robotic systems [35-38]. Abbott and Okamura [39] have presented an impedance model (with a damping element) for the master and slave robots by employing a PD controller.

In order to perform dexterous resistive/assistive tele-rehabilitation task using multi-DOF teleoperation systems, a stable nonlinear bilateral impedance control strategy is designed in this work considering the patient and therapist characteristics. Note that the patient should apply forces to move his limb in a resistive therapeutic exercise; however, he can be helped as much as needed by providing an online assistive

force of therapist to successfully perform the task. Now, the comparative features and advantages of the proposed bilateral control strategy are mentioned as follows:

1. Response of a first desired virtual impedance model is tracked by the master robot (in the patient's hand). This first impedance model includes mass, damping and stiffness elements, which has a response trajectory to the combination of patient and scaled therapist forces. While the slave robot (in the therapist's hand) tracks the master trajectory plus a deviation as the response of a second virtual impedance model. This second impedance model also have mass, damping and stiffness elements, which generates the desired slave-master deviation trajectory in response to the therapist force. Accordingly, an adjustable resistive virtual impedance-based dynamics for the collaboration between the patient and the therapist is realized by the first impedance model. The second impedance model is also augmented to guarantee the absolute stability of teleoperation system. Two sources of adjustable resistance and assistance are provided in this framework: (a) the resistive dynamics of the virtual environment, which can be adjusted before the tele-rehabilitation task, and (b) the online (live) assistive force of the therapist during the task. These impedance-based control objectives are novel in comparison with the position- and force-based control objectives of previous nonlinear adaptive controllers [24-27], and have tele-rehabilitation applications.
2. Parameters of the first desired impedance model can be adjusted to amplify the patient's effort for highly impaired ones. This is achieved by increasing the effect of the patient's force in the impedance model. Moreover, parameters of the second

desired impedance model are adjusted based on the absolute stability criterion. These features were not realized by the previous adaptive controllers [26-30] with the transparency objective (position and force tracking).

3. Involuntary tremors of the patient's limb can be filtered out via appropriate adjustments of the first impedance model parameters. This characteristic is useful in rehabilitation of post-stroke patients with Cerebellar or Intention tremors [40, 41], where the voluntary forces or motions of the patient need to be distinguished from their involuntary motions. This feature is also helpful for other patients suffering from tremors due to the Cerebral Palsy (CP) and the Parkinson's disease (PD).
4. The absolute stability and Lyapunov-based tracking convergence of the nonlinear tele-robotic system subjected to time delays are proven. In this bilateral adaptive controller, robustness against modeling uncertainties in the teleoperation system is guaranteed using the proposed nonlinear adaptation laws. The communication delays between the master and slave are taken into account in order to facilitate tele-rehabilitation. The proven stability of the delayed tele-robotic system improves the patient and therapist safety during interaction with robots. Note that previous linear impedance controllers [35-39] are not suitable for the nonlinear dynamics of multi-DOF tele-robotic systems used in rehabilitation therapies.

Note that in previous adaptive position error based (PEB) bilateral control methods (e.g., [24-27]), the master robot trajectory was tracked by the slave controller and the slave robot trajectory was tracked by the master controller for the position synchronization. However, in the currently presented work, desired impedance-based

control objectives are proposed by defining two impedance models for the master and slave robots instead of position synchronization (due to the above-mentioned item 1). This proposed impedance-based bilateral controller is also designed to be suitable for the tele-rehabilitation with resistive/assistive strategy and patient-therapist collaboration (as described in items 1, 2 and 3). In addition, the stability of the closed-loop teleoperation system in the presence of communication delays is proven in this work (expressed in item 4). However, these time delays and the corresponding absolute stability were not considered in recent bilateral adaptive controllers (e.g., [27]).

2. RESISTIVE/ASSISTIVE TELE-REHABILITATION

Using a bilateral tele-robotic system, resistive/assistive tele-rehabilitation tasks can be performed employing a bilateral impedance control strategy. In this teleoperation configuration, the patient and therapist physically interact with the master and slave robots, respectively. The first proposed desired impedance model realizes the patient-therapist collaboration in a resistive virtual environment. For this purpose, the therapist-slave interaction force ($\mathbf{f}_{th}$) is transmitted to the patient-side (master robot) to be employed in the first impedance model. Also, the motion trajectory of the master robot ($\mathbf{x}_m$) is transmitted to be employed in the second desired impedance model that its response is tracked by the slave robot's adaptive controller. Time delays (T_1 and T_2) in the communication channels between the remote patient and the therapist are considered. The concepts of impedance models and delayed transmitted signals (that have a superscript of "*d*") are illustrated in Fig. 1.

2.1. Desired Impedance-based Control Objectives

The first desired impedance model represents the resistive virtual environment as a dynamical relation between a linear combination of the patient $\mathbf{f}_{pa}$ and the therapist $\mathbf{f}_{th}$ interaction forces, and the desired master robot trajectory $\mathbf{x}_{des_m}$ in the Cartesian space:

$$m_{des_m}\ddot{\mathbf{x}}_{des_m} + c_{des_m}\dot{\mathbf{x}}_{des_m} + k_{des_m}(\mathbf{x}_{des_m} - \mathbf{x}_0) = \mathbf{f}_{pa} + \mu_{\mathrm{f}}\mathbf{f}_{th}^{d} \quad (1)$$

Here, $\mathbf{x}_0$ is the neutral position of the master robot in the absence of forces (when $\mathbf{f}_{th} = \mathbf{f}_{pa} = 0$). Note that the master controller will prepare the force-position haptic sense of Eq. (1) for the patient by providing the convergence of master robot's trajectory (i.e., the patient limb's trajectory) to the response of desired impedance model (1): $\mathbf{x}_m \to \mathbf{x}_{des_m}$. According to Eq. (1), the patient senses m_{des_m}, c_{des_m} and k_{des_m} as the virtual mass, damping and stiffness parameters of the resistive impedance model, respectively, in addition the scaled interaction force of therapist $\mu_{\mathrm{f}}\mathbf{f}_{th}^{d}$ with T_2 delay. μ_{f} is the force scaling factor in (1) for the cooperation of the therapist force $\mathbf{f}_{th}^{d}$ with the patient force $\mathbf{f}_{pa}$.

The master robot tracks the response $\mathbf{x}_{des_m}$ of the first impedance model (1) in which the therapist-slave interaction force is considered to have a communication delay (T_2) for transmission to the master side as

$$\mathbf{f}_{th}^{d}(t) = \mathbf{f}_{th}(t - T_2) \quad (2)$$

The scaled master robot's motion trajectory is also transmitted to the slave side as

$$\mathbf{x}_m^d(t) = \mathbf{x}_m(t - T_1) \tag{3}$$

Here, T_1 is the communication delay for the signal transmission from the master to the slave. This delayed master/patient trajectory is employed in the second desired impedance model that $\mathbf{x}_{des_s}$ in its response is tracked by the slave robot under the therapist's hand:

$$m_{des_s}(\ddot{\mathbf{x}}_{des_s} - \mu_{\mathrm{p}}\ddot{\mathbf{x}}_m^d) + c_{des_s}(\dot{\mathbf{x}}_{des_s} - \mu_{\mathrm{p}}\dot{\mathbf{x}}_m^d) + k_{des_s}(\mathbf{x}_{des_s} - \mu_{\mathrm{p}}\mathbf{x}_m^d) = \mathbf{f}_{th} \tag{4}$$

where μ_{p} is the position scaling factor. Although, this second impedance model (4) generates a deviation ($\mathbf{x}_{des_s} - \mu_{\mathrm{p}}\mathbf{x}_m^d$) for the desired slave trajectory with respect to the scaled master trajectory in the presence of therapist force $\mathbf{f}_{th}$, it will be shown that is required for the absolute stability of delayed teleoperation system.

The response of first and second desired impedance models (1) and (4) are obtained by numerical integration of them with a fast sampling rate, and will be used in the master and slave controllers. It should be mentioned that the patient-master and therapist-slave interaction forces ($\mathbf{f}_{pa}$ and $\mathbf{f}_{th}$) are required to be measured by force sensors and employed in the impedance models (1) and (4). Thus, if the force sensors are not accurate and have measurement errors, the desired master and slave impedance models (1) and (4) are not realized well. In other words, the patient and therapist do not sense these models (1) and (4) precisely in response to their interaction forces ($\mathbf{f}_{pa}$ and $\mathbf{f}_{th}$) applied to the master and slave robots, respectively.

2.2. Resistive / Assistive Strategy

In a resistive/assistive strategy, the patient is opposed and sometimes aided to move in order to engage him in a desired task [3]. This tele-rehabilitation strategy can be implemented using the proposed bilateral impedance controller. For this purpose, the resistive impedance model elements (m_{des_m} , c_{des_m} and k_{des_m}) in (1) should have such values that the patient needs to apply significant amount of forces required for moving the virtual mass m_{des_m} , the damping c_{des_m} and the stiffness k_{des_m} even in the absence of the therapist force (when $\mathbf{f}_{th} = 0$). Accordingly, the patient (interacting with the master robot) perceives to be moving in a resistive position-, velocity- and acceleration-dependent virtual environment. The level of resistance can be adjusted by selecting the first impedance model parameters based on the therapist's opinion and the patient's motor performance. The therapist can assist the patient as much as needed during the rehabilitation task by applying the force ($\mathbf{f}_{th}$ in Eq.(1)) when he finds out that the patient cannot move and reach to target successfully in the resistive environment.

2.2.1 Patients with moderate disability

The impedance parameters in Eq. (1) should be adjusted on moderate values (e.g., $k_{des_m} = 100\ \mathrm{N/m}$) in order to realize a moderate resistive environment for the patients with moderate disability based on his motor performance. In order to reduce the level of resistance perceived by the therapist, the force scaling factor μ_{f} can be

chosen larger than 1 (e.g., $\mu_{\mathrm{f}} = 3$). This would decrease the therapist fatigue during the therapy process in the resistive virtual environment (1), and reduce the magnitude of his/her ($\mathbf{f}_{th}$) force in comparison with the patient one ($\mathbf{f}_{pa}$).

2.2.2 Severely impaired patients (need effort amplification)

The patient effort can be amplified as much as needed using the suggested control framework to more actively engage the patients with severe disabilities in the rehabilitation process. Severely impaired patients have troubles with completing common movements with sufficient force [3]. Therefore, the amplification of their forces encourages them to make an effort for moving the affected limb. Also, using this amplification, the therapist can better identify the small forces applied by the patient that indicate his intention.

Consequently, in the proposed bilateral impedance controller, if the impedance model parameters in (1) are set to be considerably small (e.g., $k_{des_m} = 20\ \mathrm{N/m}$), the first impedance model becomes highly responsive to small forces of the patient. Therefore, the effect of the patient force $\mathbf{f}_{pa}$ in Eq. (1) is magnified and the patient can move the master robot with small forces. In this condition, the force scaling factor can be $\mu_{\mathrm{f}} = 1$ in (1) to provide the same authority for the patient and therapist forces ($\mathbf{f}_{pa}$ and $\mathbf{f}_{th}^{d}$).

It should be mentioned that the suggested resistance levels and stiffness values in Sec. 2.2.1 and Sec. 2.2.2 are case-dependent and should be adjusted appropriately by a trial-and-error method in realistic rehabilitation therapies for each patient based on his motor performance and the therapist opinion.

2.2.3 Filtration of Patient Tremors

Stroke patients may experience the oscillatory Cerebellar tremor in actions, intentions and purposeful movements of their arms [40, 41]. The frequency of this rhythmic involuntary tremor is about $5\ \text{Hz}$ [40, 41] or in $4-6\ \text{Hz}$ [42], and it has large amplitudes. Also, patients with certain other diseases such as Parkinson usually have significant involuntary tremors [41].

As an interesting feature of the proposed control scheme, the patient limb tremors can be filtered out by setting the cut-off frequency ($\approx \omega_{n_{des_m}} = \sqrt{k_{des_m} / m_{des_m}}$) of the first impedance model (1) to be several times smaller than the minimum patient tremor frequency ($\omega_{trem_{\min}}$). As the magnitude Bode diagram of the first impedance model (1) in Fig. 2 shows the magnitude of $|k_{des_m} \mathbf{X}_{des_{m\ trem}} / \mathbf{F}_{pa\ trem}|$, if $\omega_{n_{des_m}} << \omega_{trem}$, the involuntary tremor-related portion of the patient forces is attenuated significantly. In this case, given (1) and based on $-40\ \text{dB/decade}$ slope of the Bode plot over frequencies higher than the natural frequency, the magnitude of the first impedance model's response $\mathbf{x}_{des_m}$ with respect to the tremor portion of the patient force $\mathbf{f}_{pa\ trem}$ is $|\mathbf{X}_{des_{m\ trem}}| \le (\omega_{trem_{\min}} / \omega_{n_{des}})^2 |\mathbf{F}_{pa_{trem}} / k_{des_m}|$. This smooth impedance model response is tracked by the master robot end-effector under the patient's hand ($\mathbf{x}_m \to \mathbf{x}_{des_m}$). Consequently, the response $\mathbf{x}_{des_s}$ of the second impedance model (4) in terms of the master trajectory $\mathbf{x}_m^d$ becomes smooth, which is tracked by the slave robot under the

therapist's hand ($\mathbf{x}_s \to \mathbf{x}_{des_s}$). This tremor elimination decreases the therapist's fatigue as well.

In summary, the patient can affect the robots trajectories via the non-oscillatory (non-tremor) voluntary part of his force. For amplification of the patient's force (Sec. 2.2.2), the elimination of the patient tremors is very important. If the patient tremor force is not filtered, a large reciprocating motion is produced in the master trajectory due to (1) and also in the slave trajectory based on (4).

The parameter adjustment of the first impedance model (1) for collaboration of the patient and therapist using the proposed bilateral impedance-controlled tele-rehabilitation system are listed in Table 1. Without loss of generality, two values are suggested for the force scaling factor (μ_{f}) in Table 1. Moreover, the position scaling factor (μ_{p}) should be specified according to the ratio of the master and slave robots' workspaces.

Note the moderate and small values (in Table 1) for the stiffness parameter are suggested to be $50 \text{ N/m} < k_{des_m} < 200 \text{ N/m}$ and $k_{des_m} < 25 \text{ N/m}$, respectively. These sample ranges also depend on the patient's and therapist's haptic senses, patient's disabilities and the workspace of rehabilitation tasks. Consequently, this impedance parameter (stiffness k_{des_m}) should be adjusted appropriately for each patient using some preliminary experimental analyses. Moreover, the damping c_{des_m} and mass m_{des_m} parameters of the first impedance model (1) can be adjusted based on the stiffness parameter k_{des_m} and other characteristics such as the natural frequency

$\omega_{n_{des_m}} = \sqrt{k_{des_m}/m_{des_m}} \leq 0.2\,\omega_{trem_{\min}}$ for tremor filtration and the chosen damping ratio $\zeta_{des_m} = c_{des_m}/2\sqrt{m_{des_m}k_{des_m}}$.

3. NONLINEAR TELE-ROBOTIC SYSTEM

The nonlinear dynamics of a tele-robotic system with multi-DOF master and slave robots is defined in the Cartesian space as [43]

$$\mathbf{M}_{\mathbf{x},m}(\mathbf{q}_m)\ddot{\mathbf{x}}_m + \mathbf{C}_{\mathbf{x},m}(\mathbf{q}_m,\dot{\mathbf{q}}_m)\dot{\mathbf{x}}_m + \mathbf{G}_{\mathbf{x},m}(\mathbf{q}_m) + \mathbf{F}_{\mathbf{x},m}(\dot{\mathbf{q}}_m) = \mathbf{f}_m + \mathbf{f}_{pa} \quad (5)$$

$$\mathbf{M}_{\mathbf{x},s}(\mathbf{q}_s)\ddot{\mathbf{x}}_s + \mathbf{C}_{\mathbf{x},s}(\mathbf{q}_s,\dot{\mathbf{q}}_s)\dot{\mathbf{x}}_s + \mathbf{G}_{\mathbf{x},s}(\mathbf{q}_s) + \mathbf{F}_{\mathbf{x},s}(\dot{\mathbf{q}}_s) = \mathbf{f}_s + \mathbf{f}_{th} \quad (6)$$

where $\mathbf{x}_m$ and $\mathbf{x}_s$ are the Cartesian position vectors of the master and slave robots' end-effectors, respectively. $\mathbf{q}_m$ and $\mathbf{q}_s$ are the joint position vectors, $\mathbf{M}_{\mathbf{x},m}(\mathbf{q}_m)$ and $\mathbf{M}_{\mathbf{x},s}(\mathbf{q}_s)$ are the inertia or mass matrices, $\mathbf{C}_{\mathbf{x},m}(\mathbf{q}_m,\dot{\mathbf{q}}_m)$ and $\mathbf{C}_{\mathbf{x},s}(\mathbf{q}_s,\dot{\mathbf{q}}_s)$ include the centrifugal and Coriolis terms, $\mathbf{G}_{\mathbf{x},m}(\mathbf{q}_m)$ and $\mathbf{G}_{\mathbf{x},s}(\mathbf{q}_s)$ are the gravity forces, $\mathbf{F}_{\mathbf{x},m}(\dot{\mathbf{q}}_m)$ and $\mathbf{F}_{\mathbf{x},s}(\dot{\mathbf{q}}_s)$ are the friction forces, and $\mathbf{f}_m$ and $\mathbf{f}_s$ are the control forces of the master and the slave robots, respectively. $\mathbf{f}_{pa}$ and $\mathbf{f}_{th}$ are the interaction forces that the patient applies to the master end-effectors and the therapist applies to the slave end-effector, respectively. Considering the subscripts $i=m$ and $i=s$ for the master and slave, respectively, the robots' dynamic matrices and vectors have the following properties [27, 43, 44]:

- The left sides of (5) and (6) can be linearly parameterized:

$$\mathbf{M}_{\mathbf{x},i}(\mathbf{q}_i)\boldsymbol{\chi}_{\mathbf{1},i} + \mathbf{C}_{\mathbf{x},i}(\mathbf{q}_i,\dot{\mathbf{q}}_i)\boldsymbol{\chi}_{\mathbf{2},i} + \mathbf{G}_{\mathbf{x},i}(\mathbf{q}_i) + \mathbf{F}_{\mathbf{x},i}(\dot{\mathbf{q}}_i) = \mathbf{R}_{\mathbf{x},i}(\chi_{1,i},\chi_{2,i},\mathbf{q}_i,\dot{\mathbf{q}}_i)\boldsymbol{\beta}_{\mathbf{x},i} \quad (7)$$

where $\mathbf{R}_{\mathbf{x},i}$ is the regressor matrix in terms of the known vectors $\boldsymbol{\chi}_{\mathbf{1},i}$ and $\boldsymbol{\chi}_{\mathbf{2},i}$, and $\boldsymbol{\beta}_{\mathbf{x},i}$ is the vector of unknown robot's parameters.

- $\mathbf{M}_{\mathbf{x},i}(\mathbf{q}_i)$ and $\dot{\mathbf{M}}_{\mathbf{x},i}(\mathbf{q}_i) - 2\mathbf{C}_{\mathbf{x},i}(\mathbf{q}_i, \dot{\mathbf{q}}_i)$ are symmetric positive definite and skew symmetric matrices, respectively.

4. NONLINEAR BILATERAL ADAPTIVE CONTROL OF MASTER AND SLAVE ROBOTS

The block diagram of the proposed nonlinear bilateral adaptive controller with two desired impedance models and delayed communication channels are shown in Fig. 3. As stated in Sec. 2.1, the desired impedance models (1) and (4) are realized for the master and slave robots employing a nonlinear bilateral control method. In this controller, the response of first impedance model (1) is tracked by the master robot and the slave robot also tracks the master trajectory plus the response of second impedance model (4). Communication delays (T_1 and T_2) are taken into account between the master-patient and slave-therapist sites.

In order to design the nonlinear bilateral controller for the multi-DOF robotic tele-rehabilitation system, the master and slave sliding surfaces are defined as

$$\boldsymbol{\varepsilon}_m = \dot{\tilde{\mathbf{x}}}_m + \alpha_{1,m}\tilde{\mathbf{x}}_m + \alpha_{2,m}\int_0^t \tilde{\mathbf{x}}_m\, dt\,, \qquad \boldsymbol{\varepsilon}_s = \dot{\tilde{\mathbf{x}}}_s + \alpha_{1,s}\tilde{\mathbf{x}}_s + \alpha_{2,s}\int_0^t \tilde{\mathbf{x}}_s\, dt \tag{8}$$

where $\tilde{\mathbf{x}}_m = \mathbf{x}_m - \mathbf{x}_{des_m}$ and $\tilde{\mathbf{x}}_s = \mathbf{x}_s - \mathbf{x}_{des_s}$ are the master and slave position tracking errors with respect to their desired trajectories described in Sec. 2.1. $\alpha_{1,m}$, $\alpha_{2,m}$, $\alpha_{1,s}$ and $\alpha_{2,s}$ are positive constant parameters that guarantee the stability of the sliding

surfaces, i.e. $\tilde{\mathbf{x}}_i \to 0$ as $\boldsymbol{\varepsilon}_i \to 0$ for $i = m, s$. The master and slave reference velocities $\dot{\mathbf{x}}_{ref,m}$ and $\dot{\mathbf{x}}_{ref,s}$ are represented such that the sliding surfaces (8) can be rewritten as $\boldsymbol{\varepsilon}_m = \dot{\mathbf{x}}_m - \dot{\mathbf{x}}_{ref,m}$ and $\boldsymbol{\varepsilon}_s = \dot{\mathbf{x}}_s - \dot{\mathbf{x}}_{ref,s}$:

$$\dot{\mathbf{x}}_{ref,m} = \dot{\mathbf{x}}_{des_m} - \alpha_{1,m}\tilde{\mathbf{x}}_m - \alpha_{2,m}\int_0^t \tilde{\mathbf{x}}_m\, dt, \qquad \dot{\mathbf{x}}_{ref,s} = \dot{\mathbf{x}}_{des_s} - \alpha_{1,s}\tilde{\mathbf{x}}_s - \alpha_{2,s}\int_0^t \tilde{\mathbf{x}}_s\, dt \tag{9}$$

Now, the nonlinear adaptive control laws for the master and slave robots are proposed as

$$\begin{aligned}\mathbf{f}_m = {} & \hat{\mathbf{M}}_{\mathbf{x},m}(\mathbf{q}_m)\ddot{\mathbf{x}}_{ref,m} - \alpha_{3,m}\hat{\mathbf{M}}_{\mathbf{x},m}(\mathbf{q}_m)\boldsymbol{\varepsilon}_m \\ & + \hat{\mathbf{C}}_{\mathbf{x},m}(\mathbf{q}_m,\dot{\mathbf{q}}_m)\dot{\mathbf{x}}_{ref,m} + \hat{\mathbf{G}}_{\mathbf{x},m}(\mathbf{q}_m) + \hat{\mathbf{F}}_{\mathbf{x},m}(\dot{\mathbf{q}}_m) - \mathbf{f}_{pa}\end{aligned} \tag{10}$$

$$\begin{aligned}\mathbf{f}_s = {} & \hat{\mathbf{M}}_{\mathbf{x},s}(\mathbf{q}_s)\ddot{\mathbf{x}}_{ref,s} - \alpha_{3,s}\hat{\mathbf{M}}_{\mathbf{x},s}(\mathbf{q}_s)\boldsymbol{\varepsilon}_s \\ & + \hat{\mathbf{C}}_{\mathbf{x},s}(\mathbf{q}_s,\dot{\mathbf{q}}_s)\dot{\mathbf{x}}_{ref,s} + \hat{\mathbf{G}}_{\mathbf{x},s}(\mathbf{q}_s) + \hat{\mathbf{F}}_{\mathbf{x},s}(\dot{\mathbf{q}}_s) - \mathbf{f}_{th}\end{aligned} \tag{11}$$

where $\wedge$ is used for the estimated or updated values of vectors and matrices. $\alpha_{3,m}$ and $\alpha_{3,s}$ are positive constant parameters that guarantee the Lyapunov stability of master and slave closed-loop dynamics ($\boldsymbol{\varepsilon}_i \to 0$ for $i = m, s$), as proven in Sec. 5. According to the mentioned property (7) in Sec. 3, the control laws (10) and (11) can be represented in a linearly parameterized form as

$$\mathbf{f}_m = \mathbf{R}_{\mathbf{x},m}\hat{\boldsymbol{\beta}}_{\mathbf{x},m} - \mathbf{f}_{pa} \quad , \qquad \mathbf{f}_s = \mathbf{R}_{\mathbf{x},s}\hat{\boldsymbol{\beta}}_{\mathbf{x},s} - \mathbf{f}_{th} \tag{12}$$

where $\mathbf{R}_{\mathbf{x},m}$ and $\mathbf{R}_{\mathbf{x},s}$ are the regressor matrices determined by Eq. (7) in terms of the following known vectors:

$$\boldsymbol{\chi}_{\mathbf{1},m} = \ddot{\mathbf{x}}_{ref,m} - \alpha_{3,m}\,\boldsymbol{\varepsilon}_m, \quad \boldsymbol{\chi}_{\mathbf{2},m} = \dot{\mathbf{x}}_{ref,m}, \quad \boldsymbol{\chi}_{\mathbf{1},s} = \ddot{\mathbf{x}}_{ref,s} - \alpha_{3,s}\,\boldsymbol{\varepsilon}_s, \quad \boldsymbol{\chi}_{\mathbf{2},s} = \dot{\mathbf{x}}_{ref,s} \tag{13}$$

Note that the control torques applied in the joint space by servo motors are obtained in terms of master and slave Jacobian matrices ($\mathbf{J}_m(\mathbf{q}_m)$, $\mathbf{J}_s(\mathbf{q}_s)$) and the Cartesian control laws (12) as $\boldsymbol{\tau}_m = \mathbf{J}_m^T \mathbf{f}_m$ and $\boldsymbol{\tau}_s = \mathbf{J}_s^T \mathbf{f}_s$.

In order to obtain the closed-loop dynamics of the master and slave robots, the control laws (10) and (11) or (12) are substituted in the tele-robotic system's dynamics (5) and (6). The result of this substitution yields the following equations after some steps that are presented in the Appendix:

$$\mathbf{M}_{\mathbf{x},m}\dot{\boldsymbol{\varepsilon}}_m + \alpha_{3,m}\mathbf{M}_{\mathbf{x},m}\boldsymbol{\varepsilon}_m + \mathbf{C}_{\mathbf{x},m}\boldsymbol{\varepsilon}_m = \mathbf{R}_{\mathbf{x},m}\tilde{\boldsymbol{\beta}}_{\mathbf{x},m} \tag{14}$$

$$\mathbf{M}_{\mathbf{x},s}\dot{\boldsymbol{\varepsilon}}_s + \alpha_{3,s}\mathbf{M}_{\mathbf{x},s}\boldsymbol{\varepsilon}_s + \mathbf{C}_{\mathbf{x},s}\boldsymbol{\varepsilon}_s = \mathbf{R}_{\mathbf{x},s}\tilde{\boldsymbol{\beta}}_{\mathbf{x},s} \tag{15}$$

where $\tilde{\boldsymbol{\beta}}_{\mathbf{x},m} = \hat{\boldsymbol{\beta}}_{\mathbf{x},m} - \boldsymbol{\beta}_{\mathbf{x},m}$ and $\tilde{\boldsymbol{\beta}}_{\mathbf{x},s} = \hat{\boldsymbol{\beta}}_{\mathbf{x},s} - \boldsymbol{\beta}_{\mathbf{x},s}$ are the parameter estimation errors of the master and slave dynamics, respectively.

It should be emphasized that accurate force sensors are required to measure interaction forces ($\mathbf{f}_{pa}$ and $\mathbf{f}_{th}$) and employ them in the control laws (10) and (11). However, if these measurements have bounded errors ($\mathbf{f}_{pa} - \hat{\mathbf{f}}_{pa}$ and $\mathbf{f}_{th} - \hat{\mathbf{f}}_{th}$), the proposed controller should become robust against this unstructured uncertainty in the master and slave closed-loop dynamics. Due to the nonlinear structure of the proposed strategy, new SMC[2] terms $-\gamma_m \operatorname{sgn}(\boldsymbol{\varepsilon}_m)$ and $-\gamma_s \operatorname{sgn}(\boldsymbol{\varepsilon}_s)$ [43] can be added to the control laws (10) and (11), respectively, such that the system becomes robust against the bounded force measurement errors $(\tilde{\mathbf{f}}_{pa} = \mathbf{f}_{pa} - \hat{\mathbf{f}}_{pa})$ and $(\tilde{\mathbf{f}}_{th} = \mathbf{f}_{th} - \hat{\mathbf{f}}_{th})$. Note that the positive constant gains γ_m and γ_s of the above-mentioned SMC terms should be

[2] Sliding Mode Control [43]

adjusted larger than the maximum values of the force measurement errors $\tilde{\mathbf{f}}_{pa}$ and $\tilde{\mathbf{f}}_{th}$, respectively (if the stability analysis is presented). In this work, due to the employment of accurate force sensors, these uncertainties are not studied in more detail.

5. LYAPUNOV-BASED CONVERGENCE PROOF FOR TELE-ROBOTIC SYSTEM

Now, the convergence of the controlled nonlinear tele-robotic system to desired trajectories ($\mathbf{x}_m \to \mathbf{x}_{des_m}$ and $\mathbf{x}_s \to \mathbf{x}_{des_s}$) for the tele-rehabilitation is investigated in the presence of modeling uncertainties. For this purpose, a positive definite Lyapunov function is employed as

$$V(t) = \frac{1}{2}\left(\boldsymbol{\varepsilon}_m^T \mathbf{M}_{\mathbf{x},m}\boldsymbol{\varepsilon}_m + \tilde{\boldsymbol{\beta}}_{\mathbf{x},m}^T \boldsymbol{\Psi}_m^{-1}\tilde{\boldsymbol{\beta}}_{\mathbf{x},m} + \boldsymbol{\varepsilon}_s^T \mathbf{M}_{\mathbf{x},s}\boldsymbol{\varepsilon}_s + \tilde{\boldsymbol{\beta}}_{\mathbf{x},s}^T \boldsymbol{\Psi}_s^{-1}\tilde{\boldsymbol{\beta}}_{\mathbf{x},s}\right) \tag{16}$$

where $\boldsymbol{\Psi}_m$ and $\boldsymbol{\Psi}_s$ are constant positive definite matrices that will be used in the adaptation laws. The first time derivative of the Lyapunov function (16) is determined as

$$\begin{aligned}\dot{V}(t) = {} & (1/2)\boldsymbol{\varepsilon}_m^T \dot{\mathbf{M}}_{\mathbf{x},m}\boldsymbol{\varepsilon}_m + \boldsymbol{\varepsilon}_m^T \mathbf{M}_{\mathbf{x},m}\dot{\boldsymbol{\varepsilon}}_m + \dot{\hat{\boldsymbol{\beta}}}_{\mathbf{x},m}^T \boldsymbol{\Psi}_m^{-1}\tilde{\boldsymbol{\beta}}_{\mathbf{x},m} \\ & + (1/2)\boldsymbol{\varepsilon}_s^T \dot{\mathbf{M}}_{\mathbf{x},s}\boldsymbol{\varepsilon}_s + \boldsymbol{\varepsilon}_s^T \mathbf{M}_{\mathbf{x},s}\dot{\boldsymbol{\varepsilon}}_s + \dot{\hat{\boldsymbol{\beta}}}_{\mathbf{x},s}^T \boldsymbol{\Psi}_s^{-1}\tilde{\boldsymbol{\beta}}_{\mathbf{x},s}\end{aligned} \tag{17}$$

where $\dot{\hat{\boldsymbol{\beta}}}_{\mathbf{x},i} = \dot{\tilde{\boldsymbol{\beta}}}_{\mathbf{x},i}$ (for $i = m, s$) because $\hat{\boldsymbol{\beta}}_{\mathbf{x},i} = \tilde{\boldsymbol{\beta}}_{\mathbf{x},i} + \boldsymbol{\beta}_{\mathbf{x},i}$ and the actual robots' parameters are constant ($\dot{\boldsymbol{\beta}}_{\mathbf{x},i} = 0$). Substituting $\mathbf{M}_{\mathbf{x},m}\dot{\boldsymbol{\varepsilon}}_m$ and $\mathbf{M}_{\mathbf{x},s}\dot{\boldsymbol{\varepsilon}}_s$ from the final closed-loop dynamics of robots (14) and (15) into (17) and employing the property of the manipulators' dynamics that $\dot{\mathbf{M}}_{\mathbf{x},i} - 2\mathbf{C}_{\mathbf{x},i}$ is skew symmetric (introduced in Sec. 3), concludes:

$$\begin{aligned}\dot{V}(t) = {} & \boldsymbol{\varepsilon}_m^T \mathbf{R}_{\mathbf{x},m} \tilde{\boldsymbol{\beta}}_{\mathbf{x},m} + \dot{\hat{\boldsymbol{\beta}}}_{\mathbf{x},m}^T \boldsymbol{\Psi}_m^{-1} \tilde{\boldsymbol{\beta}}_{\mathbf{x},m} - \alpha_{3,m} \boldsymbol{\varepsilon}_m^T \mathbf{M}_{\mathbf{x},m} \boldsymbol{\varepsilon}_m \\ & + \boldsymbol{\varepsilon}_s^T \mathbf{R}_{\mathbf{x},s} \tilde{\boldsymbol{\beta}}_{\mathbf{x},s} + \dot{\hat{\boldsymbol{\beta}}}_{\mathbf{x},s}^T \boldsymbol{\Psi}_s^{-1} \tilde{\boldsymbol{\beta}}_{\mathbf{x},s} - \alpha_{3,s} \boldsymbol{\varepsilon}_s^T \mathbf{M}_{\mathbf{x},s} \boldsymbol{\varepsilon}_s\end{aligned} \tag{18}$$

Then, the nonlinear adaptation laws for updating the master and slave estimated parameters are presented as

$$\dot{\hat{\boldsymbol{\beta}}}_{\mathbf{x},m} = -\boldsymbol{\Psi}_m^T \mathbf{R}_{\mathbf{x},m}^T \boldsymbol{\varepsilon}_m \ , \qquad \dot{\hat{\boldsymbol{\beta}}}_{\mathbf{x},s} = -\boldsymbol{\Psi}_s^T \mathbf{R}_{\mathbf{x},s}^T \boldsymbol{\varepsilon}_s \tag{19}$$

by which the terms in (18) that contain $\tilde{\boldsymbol{\beta}}_{\mathbf{q},m}$ and $\tilde{\boldsymbol{\beta}}_{\mathbf{q},s}$ are cancelled. Therefore, time derivatives of the Lyapunov function (18) is finally reduced to:

$$\dot{V}(t) = -\alpha_{3,m} \boldsymbol{\varepsilon}_m^T \mathbf{M}_{\mathbf{x},m} \boldsymbol{\varepsilon}_m - \alpha_{3,s} \boldsymbol{\varepsilon}_s^T \mathbf{M}_{\mathbf{x},s} \boldsymbol{\varepsilon}_s \tag{20}$$

Since the Lyapunov function (16) is positive definite ($V(t) > 0$) and its time derivatives (20) is negative semi-definite ($\dot{V}(t) \le 0$), the boundedness of $V(t)$ is concluded. Based on the Barbalat's lemma [43], having a uniformly continuous function $g(t)$ for $t \ge 0$ such that the limit of its integral $\lim_{t\to\infty} \int_0^t g(\upsilon) d\upsilon$ exists and has a finite value, the convergence of $\lim_{t\to\infty} g(\upsilon) = 0$ is concluded. In the present study, this uniformly continuous function is considered as $g(t) = \alpha_{3,m} \boldsymbol{\varepsilon}_m^T \mathbf{M}_{\mathbf{x},m} \boldsymbol{\varepsilon}_m + \alpha_{3,s} \boldsymbol{\varepsilon}_s^T \mathbf{M}_{\mathbf{x},s} \boldsymbol{\varepsilon}_s$ such that by integrating Eq. (20), it can be written:

$$V(0) - V(\infty) \ge \lim_{t\to\infty} \int_0^t g(\upsilon) d\upsilon \tag{21}$$

Also, since $\dot{V}(t) = dV(t)/dt \le 0$ is negative according to Eq. (20), $V(0) - V(\infty) \ge 0$ is positive and finite. Consequently, $\lim_{t\to\infty} \int_0^t g(\upsilon) d\upsilon$ in (21) has a finite and positive value (due to the positiveness of $g(t)$). As result, based on the Barbalat's lemma [43], it is concluded that:

$$\lim_{t\to\infty} g(t) = \lim_{t\to\infty}\left(\alpha_{3,m}\boldsymbol{\varepsilon}_m^T \mathbf{M}_{\mathbf{x},m}\boldsymbol{\varepsilon}_m + \alpha_{3,s}\boldsymbol{\varepsilon}_s^T \mathbf{M}_{\mathbf{x},s}\boldsymbol{\varepsilon}_s\right) = 0 \tag{22}$$

Therefore, because of $\alpha_{3,m} > 0$, $\alpha_{3,s} > 0$, $\boldsymbol{\varepsilon}_m^T\mathbf{M}_{\mathbf{x},m}\boldsymbol{\varepsilon}_m \geq 0$ and $\boldsymbol{\varepsilon}_s^T\mathbf{M}_{\mathbf{x},s}\boldsymbol{\varepsilon}_s \geq 0$, Eq. (22) implies the convergence to sliding surfaces $\boldsymbol{\varepsilon}_m = 0$ and $\boldsymbol{\varepsilon}_s = 0$ as $t \to \infty$. Moreover, it is ensured from Eq. (16) that the parameter estimation errors $\tilde{\boldsymbol{\beta}}_{\mathbf{x},m}$ and $\tilde{\boldsymbol{\beta}}_{\mathbf{x},s}$ remain bounded due to the boundedness of $V(t)$.

Based on the stable dynamics of the sliding surfaces (8), convergence of the master and slave position tracking errors $\tilde{\mathbf{x}}_m \to 0$ and $\tilde{\mathbf{x}}_s \to 0$ (on the surfaces of $\boldsymbol{\varepsilon}_m = 0$ and $\boldsymbol{\varepsilon}_s = 0$) are ensured. Thus, the proposed bilateral adaptive control strategy guarantees that the master and slave robots track their corresponding desired responses of impedance models ($\mathbf{x}_m \to \mathbf{x}_{des_m}$ and $\mathbf{x}_s \to \mathbf{x}_{des_s}$) in the presence of parametric uncertainties and time-delays.

6. ABSOLUTE STABILITY OF CLOSED-LOOP TELEOPERATION SYSTEM

After proving the convergence of closed-loop nonlinear tele-robotic system to desired impedance-based trajectories ($\mathbf{x}_m \to \mathbf{x}_{des_m}$ and $\mathbf{x}_s \to \mathbf{x}_{des_s}$), the absolute stability of bilateral impedance-controlled teleoperation system is analyzed in the presence of communication delays. Absolute stability [37, 45] is a well-known criterion for the stability analysis of a teleoperation system modeled by a two-port network. For this analysis, the hybrid matrix of the proposed bilateral teleoperation system in each

Cartesian coordinate (*j*) is obtained as a result of realizing the first and second impedance models (1) and (4) as

$$\mathbf{H}_j = \begin{bmatrix} m_{des_m} s + c_{des_m} & \mu_{\mathrm{f}}.\mathrm{e}^{-T_2 s} \\ -\mu_{\mathrm{p}}.\mathrm{e}^{-T_1 s} & s/(m_{des_s} s^2 + c_{des_s} s + k_{des_s}) \end{bmatrix} \tag{23}$$

where $[F_{pa}(s),\ -V_s(s)]_j = \mathbf{H}_j\ [V_m(s),\ -F_{th}(s)]_j$ in which $F_{pa}(s)$, $F_{th}(s)$ and $V_m(s)$, $V_s(s)$ are the Laplace transforms of interaction forces f_{pa}, f_{th} and robots velocities $\dot{x}_m$, $\dot{x}_s$, respectively. The communication delays (T_1 and T_2) are considered to be constant. Note that the time delays of real communication channels are usually close to constant during a teleoperation task (such as tele-rehabilitation), as considered in this work. These communication delays can be measured online from sending and receiving times of transmitted signals as described in [46].

Regarding the above hybrid matrix (23) of the teleoperation system, conditions (a) and (b) together with the first two items ($\mathrm{Re}\left[h_{11,k}\right] \geq 0$ and $\mathrm{Re}\left[h_{22,k}\right] \geq 0$) of condition (c) for the absolute stability criterion (presented in [37, 45]) are satisfied by choosing positive impedance parameters. The third item of condition (c) for the absolute stability margin η_{AS} is obtained after simplifications as

$$\begin{aligned} \eta_{AS}(\omega) = {} & \mu_{\mathrm{p}}\mu_{\mathrm{f}}\left[\cos\left(\left(T_1 + T_2\right)\omega\right) - 1\right] \\ & + 2c_{des_m} c_{des_s} \omega^2 \Big/ \left[(k_{des_s} - m_{des_s}\omega^2)^2 + (c_{des_s}\omega)^2\right] \geq 0 \end{aligned} \tag{24}$$

Therefore, in the presence of time delays ($T_1 \neq 0$ and/or $T_2 \neq 0$), the positive impedance parameters (c_{des_m}, m_{des_s}, c_{des_s} and k_{des_s}) should be adjusted appropriately such that the inequality (24) is satisfied for all working frequencies ω. For this purpose, the partial

derivatives of η_{AS} in Eq. (24) with respect to the parameters of the second impedance model (4) are determined as

$$\frac{\partial \eta_{AS}(\omega)}{\partial m_{des_s}} = \frac{4c_{des_m}c_{des_s}\omega^4(k_{des_s} - m_{des_s}\omega^2)}{\left((k_{des_s} - m_{des_s}\omega^2)^2 + (c_{des_s}\omega)^2\right)^2} \tag{25}$$

$$\frac{\partial \eta_{AS}(\omega)}{\partial c_{des_s}} = \frac{2c_{des_m}\omega^2\left((k_{des_s} - m_{des_s}\omega^2)^2 - c_{des_s}^2\omega^2\right)}{\left((k_{des_s} - m_{des_s}\omega^2)^2 + (c_{des_s}\omega)^2\right)^2} \tag{26}$$

$$\frac{\partial \eta_{AS}(\omega)}{\partial k_{des_s}} = \frac{-4c_{des_m}c_{des_s}\omega^2(k_{des_s} - m_{des_s}\omega^2)}{\left((k_{des_s} - m_{des_s}\omega^2)^2 + (c_{des_s}\omega)^2\right)^2} \tag{27}$$

Based on Eqs. (25)-(27), the stability margin value $\eta_{AS}(\omega)$ can be increased in low ($\omega < \sqrt{k_{des_s}/m_{des_s}}$), moderate ($\frac{-c_{des_s} + \sqrt{c_{des_s}^2 + 4k_{des_s}m_{des_s}}}{2m_{des_s}} < \omega < \frac{c_{des_s} + \sqrt{c_{des_s}^2 + 4k_{des_s}m_{des_s}}}{2m_{des_s}}$) and high ($\omega > \sqrt{k_{des_s}/m_{des_s}}$) frequencies by decreasing the stiffness k_{des_s}, damping c_{des_s} and mass m_{des_s} parameters of the second impedance model (4), respectively, such that the inequality (24) is satisfied. Note that the parameters of the first impedance model (including c_{des_m}) are adjusted based on the resistive/assistive strategy and the patient characteristics (discussed in Sec. 2.2), regardless of the absolute stability condition (24).

7. EXPERIMENTS WITH HEALTHY HUMAN OPERATORS

The proposed resistive/assistive tele-rehabilitation strategy is evaluated using some experiments on an impedance-controlled tele-robotic system. In this experimental set-up (Fig. 4), a 2-DOF Quanser Rehab Robot (Quanser Consulting Inc., Canada)

designed for the physical rehabilitation of the upper limb is used as the master robot for interaction with the patient. On the other side, a 3-DOF Phantom Premium robot (Geomagic Inc., USA) is employed as the slave robot to interact with the therapist (Fig. 4). To measure the applied interaction forces, the Quanser Rehab and Phantom Premium robots are equipped with the ATI Gamma and ATI Nano43 force/torque sensors (ATI Industrial Automation, USA), respectively. Utilizing UDP-based communication channels between the master and the slave robots, the position and force data is transmitted. The QUARC (Quanser Real-Time Control) software is employed for implementation of the proposed nonlinear bilateral adaptive controller with a sampling time of $1\ m\text{sec}$. A two-axis accelerometer ADXL-203 (Analog Devices, Norwood, MA, USA) is attached to the master (Quanser) robot end-effector to measure its acceleration $\ddot{\mathbf{x}}_m$ which is used in the slave impedance model (4).

A reaching task is designed with some static targets, where two healthy operators act as the patient and therapist. As illustrated in Fig. 4, each operator has a monitor to observe both robots positions with respect to the target point in the $x-y$ Cartesian space. The positions of the master (or therapist), the slave (or patient), and the target point are demonstrated in the screens by the red square, blue circle and yellow circle, respectively. In these experiments, the initial states of the master and slave robots are zero, the same as responses of the impedance models (1) and (4). In other words, the operation starts form the rest configuration of robots.

The healthy human operators have become familiar with the teleoperation system by performing some initial trials and then behave as the patient and therapist in

the main following experiments. The parameters of the impedance model (1) are appropriately adjusted in the performed initial experiments based on the guidelines presented in Sec. 2 and listed in Table 1. On the other hand, the parameters of the second impedance model (4) are adjusted based on the guidelines presented in Sec.6 such that the absolute stability in the presence of communication delays is guaranteed.

7.1 With Communication Delays

In the first experiments, the transmitted force and position signals through the communication channels (shown in Figs. 1 and 3) have constant time-delays of $T_1 = 150\ m\sec$ and $T_2 = 150\ m\sec$. These time-delays are implemented by the delay block in the real-time QUARC software. The parameters of the first desired impedance model (1) are adjusted and listed in Table 2 for resistive/assistive tele-rehabilitation with different patient capabilities, as described in Sec. 2.

The stiffness parameter of the first impedance model (k_{des_m}) is adjusted based on the patient capability as discussed in Sec. 2.2. The damping ratio of the first impedance model (1) is chosen $\zeta_{des_m} = c_{des_m} \big/ 2\sqrt{m_{des_m} k_{des_m}} = 0.7$ such that it has a fast response with minimum overshoot.

The natural frequency of the impedance model (the cut-off frequency when $\zeta_{des_m} = 0.7$) is specified such that the patient's tremors are filtered out. For this purpose, $\omega_{n_{des_m}} < 0.2\,\omega_{trem_{\min}}$ is satisfied as discussed in Sec. 2.2.3. Therefore, considering the minimum frequency of the post-stroke patients Cerebellar tremors to be $\omega_{trem_{\min}} = 2\pi(1.6\ \text{Hz}) = 10.05\ \text{rad/sec}$ [42], the natural frequency of the first impedance

model (1) is chosen to be $\omega_{n_{des_m}} = \sqrt{k_{des_m} / m_{des_m}} = 2$ rad/sec. In addition, the force scaling factor μ_{f} is chosen according to the resistance level of the impedance model (magnitudes of k_{des_m}, c_{des_m} and m_{des_m}) sensed by the therapist, as discussed in Sec. 2.2.

However, the parameters (k_{des_s}, c_{des_s} and m_{des_s}) of the second impedance model (4) are adjusted such that the absolute stability criterion (24) is satisfied in the presence of time delays $T_1 = 150\ m\mathrm{sec}$ and $T_2 = 150\ m\mathrm{sec}$ for all frequency intervals described in Sec. 6. The values of impedance parameters and factors are summarized in Table 2.

Note that the parameters (k_{des_s}, c_{des_s} and m_{des_s}) of the second impedance model are adjusted on different values in Table 2 for two cases of patients in tele-rehabilitation. This is due to the different values of the damping parameter (c_{des_m}) and the force scaling factor (μ_{f}) selected for the first impedance model in these cases, which affect the obtained absolute stability condition (24). In other words, using different values of c_{des_m} and μ_{f} for the first impedance model (1) resulted in different values of k_{des_s}, c_{des_s} and m_{des_s} in the second impedance model (4) such that the stability condition (24) is satisfied in each case.

The 3-DOF master robot is controlled to have motions in the two dimensional $x-y$ plane that includes the slave robot's workspace. The kinematics and dynamics of the master and slave (Phantom and Quanser) robots were described in [47] and [48, 49], respectively.

For the resistive/assistive tele-rehabilitation, a point-to-point reaching task is provided for the therapist and patient with a visual feedback. For this purpose, 8 static target points in different positions of the $x-y$ plane are visually demonstrated with yellow circle that are changed one by one after each successful attainment of the patient to each target and returning to the origin ($\mathbf{x}_0=[0,0]^{\mathrm{T}}$). The positions of these sequenced 8 target points are: $\mathbf{x}_{t1}=[0\,m,0.07\,m]^{\mathrm{T}}$, $\mathbf{x}_{t2}=[0.07\,m,0\,m]^{\mathrm{T}}$, $\mathbf{x}_{t3}=[0,-0.07\,m]^{\mathrm{T}}$, $\mathbf{x}_{t4}=[-0.07\,m,0\,m]^{\mathrm{T}}$, $\mathbf{x}_{t5}=[0.05\,m,0.05\,m]^{\mathrm{T}}$, $\mathbf{x}_{t6}=[0.05\,m,-0.05\,m]^{\mathrm{T}}$, $\mathbf{x}_{t7}=[-0.05\,m,-0.05\,m]^{\mathrm{T}}$, $\mathbf{x}_{t8}=[-0.05\,m,0.05\,m]^{\mathrm{T}}$, respectively.

The performance of the proposed bilateral impedance controller in filtration of the hand tremors is also evaluated in these tasks. For this purpose, a healthy human operator behaves as a patient by simulating significant hand tremors (with the frequency of $4-6$ Hz [40-42]) in his purposeful movements, similar to post-stroke persons. Moreover, this able-bodied operator has applied moderate and small levels of forces toward the target points in order to simulate moderately and severely impaired patients behaviors, respectively.

7.1.1 Patient with moderate disability

As discussed in Sec. 2.2.1, the first impedance parameters k_{des_m}, c_{des_m} and m_{des_m} with moderate values (Table 2) realize the virtual resistive dynamics for the simulated patient and therapist during the tele-rehabilitation process. To make this virtual

environment less resistive for the therapist in comparison with the patient, the scaling factor of the therapist force in Eq. (1) is set on $\mu_{\mathrm{f}} = 3$.

In this case, regarding Fig. 5, the patient needs to apply the required forces for reaching to the target points due to the significant resistive virtual dynamics (1). Also, the patient has to increase his force as getting away from the origin ($\mathbf{x}_0$) and approaching the target point due to the resistance force of the stiffness k_{des_m} in Eq. (1). Therefore, the last portions of reaching to each target point would be hard for the patient to be completed because it requires larger forces. Accordingly, the therapist assists the patient as much as needed especially in the last portion of each reaching movement by applying the force ($\mathbf{f}_{th}$). The increases of therapist force at the mentioned portions of the time are highlighted by some circles in Fig. 5.

The simulated reciprocating tremor forces of the patient are seen in Fig. 5. Also, Fig. 6 shows the position responses of the master (patient) and the slave (therapist) with respect to the desired impedance models' responses. As seen, the master and slave trajectories track the first and second impedance responses ($\mathbf{x}_m \to \mathbf{x}_{des_m}$ and $\mathbf{x}_s \to \mathbf{x}_{des_s}$).

However, there is a bounded non-zero error in Fig. 6 between the master and desired slave trajectories ($\mathbf{x}_s - \mu_{\mathrm{p}} \mathbf{x}_m^d$) when the therapist applies his force $\mathbf{f}_{th}$ due to the parameter adjustment of second impedance model (4) for the absolute stability of teleoperation system in the presence of time delays ($T_1 = 150\ m\mathrm{sec}$ and $T_2 = 150\ m\mathrm{sec}$). Note that the small assistive forces of the therapist (Fig. 5) generate small deviations between the master and slave trajectories in some periods of task based on Eq. (4). These

deviations ($\mathbf{x}_s - \mu_{\mathrm{p}}\mathbf{x}_m^d$) together with convergent tracking errors ($\tilde{\mathbf{x}}_m = \mathbf{x}_m - \mathbf{x}_{des_m}$ and $\tilde{\mathbf{x}}_s = \mathbf{x}_s - \mathbf{x}_{des_s}$) are shown in Fig. 7 for x and y directions.

As an important characteristic of the proposed bilateral impedance-based tele-rehabilitation system, the reciprocating part of the patient forces (Fig. 5) that corresponds to the upper-limb tremors is filtered out. This can be found out from the desired response ($\mathbf{x}_{des_m}$) of the first impedance model (in Fig. 6) affected by the patient force ($\mathbf{f}_{pa}$). This impedance response is tracked by the master robot and the master trajectory plus a bounded deviation ($\mathbf{x}_{des_s} - \mu_{\mathrm{p}}\mathbf{x}_m^d$ as the response of second impedance model) is also tracked by the slave robot (as shown in Figs. 6 and 7). Consequently, the tremor is filtered for the patient and therapist using the proposed impedance-controlled tele-robotic system.

The trajectories of the therapist, the patient, and the desired impedance responses in $x-y$ plane are demonstrated in Fig. 8 which shows approaching to 8 target points.

7.1.2 Severely impaired patient

In this part, the proposed strategy is evaluated for the effort amplification of the patients with high levels of disability. These patients have low capability of applying forces; thus, the effectiveness of the patient force needs to be amplified by decreasing the parameters k_{des_m} , c_{des_m} and m_{des_m} in the first impedance model (1) as mentioned in Table 1. In this case, the patient (simulated by a healthy operator) becomes enabled to

move his limb together with the master robot by small forces. Therefore, the patient is encouraged to engage in the therapy process, and also the therapist can better identify the intention of (i.e., forces applied by) the patient.

Accordingly, the parameters of the first impedance model are considered to have appropriate minimum values for each trial just enough to help the patient to approach the targets; however, he may not successfully reach each target and requires more help, which is provided by the therapist's assistive force $\mu_f \mathbf{f}_{th}$. The impedance parameters and the scaling factors for this case are listed in Table 2. The parameters of the second impedance model (k_{des_s}, c_{des_s} and m_{des_s} in Table 2) are also adjusted in this case such that the absolute stability condition (24) is satisfied.

The position trajectories of the master (patient), slave (therapist) and corresponding impedance models responses in approaching the 8 targets are shown in Fig. 9 for x and y directions. The patient and therapist interaction forces are also illustrated in Fig. 10.

The assistive force of the therapist is highlighted by some red circles in Fig. 10, which helps the patient to successfully reach the targets. Since the force magnitude of a severely impaired patient in this case (Fig. 10) is considerably smaller than the one for a patient with moderate disability in the previous case (Fig. 5), the high-frequency tremor-related force consists a larger portion of the patient force in this case. Therefore, the filtration of this involuntary high-frequency part and identifying the patient's voluntary intention force is more important in this case (for a severely impaired patient). Accordingly, as seen in Figs. 9 and 10, the tremor-related force of the patient is

significantly filtered out and did not significantly affect the robots responses (patient and therapist motion trajectories) due to the adjustment of impedance model (1) in the frequency domain.

The position deviation of the slave (therapist) from the master (patient) trajectory, and the master and slave tracking errors are shown in Fig. 11. Note that the remaining bounded position error between the master and slave ($\mathbf{x}_s - \mu_{\mathrm{p}}\mathbf{x}_m^d$) is due to the adjustment of k_{des_s} , c_{des_s} and m_{des_s} in Table 2 for Eq. (4) and corresponds to the times that the therapist applies his assistive force $\mathbf{f}_{th}$ during the reaching task. It should be mentioned that the magnitude of therapist force $\mathbf{f}_{th}$ in this case (severely impaired patient) in Fig. 10 is less than the one applied in the previous case (patient with moderate disability) in Fig. 5. This is because the resistance of virtual environment is less in this case, compared with the previous case, by employing smaller parameters in the first impedance model (k_{des_m} , c_{des_m} and m_{des_m} in Table 2). However, the master-slave position error ($\mathbf{x}_s - \mu_{\mathrm{p}}\mathbf{x}_m^d$) does not change considerably in this case (Fig. 11) in comparison with the previous case (Fig. 7) due to the smaller adjusted parameters (k_{des_s} , c_{des_s} and m_{des_s} in Table 2) for the second impedance model (4) in this case.

7.2 Without Communication Delays

In this part of experiments, the communication channels are considered to be delay-free ($T_1 = T_2 = 0$). The parameters of the second impedance model (4) should be adjusted such that the absolute stability is guaranteed as discussed in Sec. 6. However,

in the absence of time-delays ($T_1 = T_2 = 0$), the absolute stability condition (24) is satisfied with arbitrary but positive parameters of the second impedance model. Therefore, these parameters are adjusted on large values as $k_{des_s} = 1000$ N/m, $c_{des_s} = 700$ N.s/m and $m_{des_s} = 250$ kg in this section instead of ones presented in Table 2 for delayed teleoperation system (Sec. 7.1). Accordingly, the slave deviation from the master trajectory ($\mathbf{x}_{des_s} - \mu_{\mathrm{p}} \mathbf{x}_m^d$) becomes considerably small as the response of Eq. (4) with respect to the bounded force $\mathbf{f}_{th}$ of the therapist. The parameters of the first impedance model (k_{des_m} , c_{des_m} , m_{des_m}) and the scaling factors (μ_{f} , μ_{p}) are chosen the same as ones presented in Sec. 7.1 (Table 2), regardless of the time-delays and the absolute stability.

Figure 12 shows the performance of delay-free teleoperation system in resistive/assistive rehabilitation of a patient with moderate disability and hand tremors. As seen in Fig. 12a, the patient applies the required forces for reaching to the target points in the resistive virtual environment defined by Eq. (1). Similar to previous experiments, the therapist assists the patient as much as needed especially in the last portion of each reaching movement by applying the force ($\mathbf{f}_{th}$). However, the slave position deviation with respect to the master trajectory ($\mathbf{x}_s - \mu_{\mathrm{p}} \mathbf{x}_m^d$) becomes small in this experiment as shown in Figs. 12b and 12c in comparison with previous experiments (Figs. 6 and 7) that performed in the presence of communication delays. This better performance in master-slave position synchronization is due to the absence of delays and consequently employing large parameters (k_{des_s} , c_{des_s} , m_{des_s}) in the second

impedance model that are not restricted by the stability condition (24) when $T_1 = T_2 = 0$. The master and slave tracking errors ($\tilde{\mathbf{x}}_m = \mathbf{x}_m - \mathbf{x}_{des_m}$ and $\tilde{\mathbf{x}}_s = \mathbf{x}_s - \mathbf{x}_{des_s}$) are also observed in Figs. 12b and 12c that converge to zero as proven in the Lyapunov analysis (Sec. 5).

Moreover, the $x-y$ trajectories of the patient, the therapist and corresponding impedance models responses in approaching the 8 targets are demonstrated in Fig. 13 for this delay-free case. As seen, the master-slave position error decreases in comparison with the one obtained in the delayed teleoperation (Fig. 8) due to the different adjustment of impedance parameters k_{des_s}, c_{des_s} and m_{des_s}.

Based on the experimental results, the presence of communication delays caused that a bounded position deviation is generated between the master and slave robots due to the parameter adjustment of the second impedance model (4) for satisfying the absolute stability condition (24). Also, the resistive/assistive strategy with some useful features (presented in Sec. 2.2) are realized by adjusting the first impedance model (1), regardless of time-delays.

8. CONCLUDING REMARKS

In this work, an impedance-based resistive/assistive tele-rehabilitation strategy was designed and implemented using nonlinear bilateral adaptive control of a tele-robotic system. Using the proposed strategy, the patient can perform a rehabilitation task in a resistive virtual environment by interacting with the master robot and with online assistance of the therapist forces applied to the slave robot. This remote patient-

therapist collaboration was realized by defining the first desired impedance model whose response was tracked by the master robot. Moreover, the slave robot tracked the master trajectory plus the response of the second impedance model.

The convergence of robots trajectories to desired responses in the presence of modeling uncertainties of master and slave robots was proven using a Lyapunov-based analysis. The absolute stability condition of teleoperation system in the presence of bounded communication delays between the patient and the therapist was investigated.

The parameters of the first desired impedance model should be adjusted based on the level of the patient's disability and his symptoms. The proposed strategy has the capability of patient tremor filtration through regulation of the first desired impedance model in the frequency domain. Moreover, the proposed framework allows for the small intention forces of severely impaired patients to be amplified to encourage them to move their disable limbs and engage them in the therapy process. Potentially small-magnitude patient intention forces can be distinguished from the involuntary tremor-related part and identified better by the therapist as a result of these force amplification and filtration features.

The parameters of the second impedance model were also adjusted appropriately to satisfy the absolute stability condition in terms of the bounded time-delays. This adjustment resulted in a bounded slave deviation from the master trajectory in delayed teleoperation systems.

The presented experimental studies using the Quanser Rehab and Phantom Premium robots showed the stability of the proposed impedance-controlled teleoperation system and its performance in realizing the desired patient-therapist collaboration with the above-mentioned features (force amplification and involuntary tremor filtration). A point-to-point reaching task with 8 static targets was designed and performed successfully with different adjustment of impedance parameters based on the patient capability, with and without communication delays.

The proposed resistive/assistive robotic tele-rehabilitation strategy was developed, analyzed and tested in this work based on an engineering point of view, where a healthy operator behaved as the patient. However, the behavior of a realistic post-stroke patient may be different from a healthy person in more detail, and effectiveness of the proposed bilateral teleoperation system can be evaluated in future clinical studies. Due to the consideration of communication delays in the stability analysis, the proposed teleoperation system can be used in realistic home-based therapy of remote patients.

In future studies, the parameters of the impedance-based virtual environment can be considered to be time-varying and autonomously adapted during the rehabilitation process based on an online analysis of the patient behavior. However, this impedance adaptation should be performed such that the stability of teleoperation system is still guaranteed. Moreover, the stability and performance of the proposed bilateral control method in the presence of varying time-delays can be studied in future works, while constant communication delays were considered in this work.

APPENDIX: MASTER AND SLAVE CLOSED-LOOP DYNAMICS

The closed-loop dynamics of the master and slave robots is obtained by employing the control laws (10) and (11) or (12) in the tele-robotic system's dynamics (5) and (6), which can be written after adding and subtracting some terms as:

$$\begin{aligned}&\mathbf{M}_{\mathbf{x},m}\ddot{\mathbf{x}}_m+\mathbf{C}_{\mathbf{x},m}\dot{\mathbf{x}}_m+\mathbf{G}_{\mathbf{x},m}+\mathbf{F}_{\mathbf{x},m}=\\&\quad\mathbf{M}_{\mathbf{x},m}(\ddot{\mathbf{x}}_{ref,m}-\alpha_{3,m}\boldsymbol{\varepsilon}_m)+\mathbf{C}_{\mathbf{x},m}\dot{\mathbf{x}}_{ref,m}+\mathbf{G}_{\mathbf{x},m}+\mathbf{F}_{\mathbf{x},m}\\&\quad+(\hat{\mathbf{M}}_{\mathbf{x},m}-\mathbf{M}_{\mathbf{x},m})(\ddot{\mathbf{x}}_{ref,m}-\alpha_{3,m}\boldsymbol{\varepsilon}_m)+(\hat{\mathbf{C}}_{\mathbf{x},m}-\mathbf{C}_{\mathbf{x},m})\dot{\mathbf{x}}_{ref,m}\\&\quad+(\hat{\mathbf{G}}_{\mathbf{x},m}-\mathbf{G}_{\mathbf{x},m})+(\hat{\mathbf{F}}_{\mathbf{x},m}-\hat{\mathbf{F}}_{\mathbf{x},m})\end{aligned}\tag{A1}$$

$$\begin{aligned}&\mathbf{M}_{\mathbf{x},s}\ddot{\mathbf{x}}_s+\mathbf{C}_{\mathbf{x},s}\dot{\mathbf{x}}_s+\mathbf{G}_{\mathbf{x},s}+\mathbf{F}_{\mathbf{x},s}=\\&\quad\mathbf{M}_{\mathbf{x},s}(\ddot{\mathbf{x}}_{ref,s}-\alpha_{3,s}\boldsymbol{\varepsilon}_s)+\mathbf{C}_{\mathbf{x},s}\dot{\mathbf{x}}_{ref,s}+\mathbf{G}_{\mathbf{x},s}+\mathbf{F}_{\mathbf{x},s}\\&\quad+(\hat{\mathbf{M}}_{\mathbf{x},s}-\mathbf{M}_{\mathbf{x},s})(\ddot{\mathbf{x}}_{ref,s}-\alpha_{3,s}\boldsymbol{\varepsilon}_s)+(\hat{\mathbf{C}}_{\mathbf{x},s}-\mathbf{C}_{\mathbf{x},s})\dot{\mathbf{x}}_{ref,s}\\&\quad+(\hat{\mathbf{G}}_{\mathbf{x},s}-\mathbf{G}_{\mathbf{x},s})+(\hat{\mathbf{F}}_{\mathbf{x},s}-\hat{\mathbf{F}}_{\mathbf{x},s})\end{aligned}\tag{A2}$$

Then, based on the linearly parameterization property (7) and Eq. (13), Eqs. (A1) and (A2) are simplified to:

$$\mathbf{M}_{\mathbf{x},m}\ddot{\mathbf{x}}_m+\mathbf{C}_{\mathbf{x},m}\dot{\mathbf{x}}_m=\mathbf{M}_{\mathbf{x},m}(\ddot{\mathbf{x}}_{ref,m}-\alpha_{3,m}\boldsymbol{\varepsilon}_m)+\mathbf{C}_{\mathbf{x},m}\dot{\mathbf{x}}_{ref,m}+\mathbf{R}_{\mathbf{x},m}\tilde{\boldsymbol{\beta}}_{\mathbf{x},m}\tag{A3}$$

$$\mathbf{M}_{\mathbf{x},s}\ddot{\mathbf{x}}_s+\mathbf{C}_{\mathbf{x},s}\dot{\mathbf{x}}_s=\mathbf{M}_{\mathbf{x},s}(\ddot{\mathbf{x}}_{ref,s}-\alpha_{3,s}\boldsymbol{\varepsilon}_s)+\mathbf{C}_{\mathbf{x},s}\dot{\mathbf{x}}_{ref,s}+\mathbf{R}_{\mathbf{x},s}\tilde{\boldsymbol{\beta}}_{\mathbf{x},s}\tag{A4}$$

Finally, according to the definition of the reference velocities $\dot{\mathbf{x}}_{ref,m}$ and $\dot{\mathbf{x}}_{ref,s}$ in Eq. (9), the closed-loop dynamics of the master and slave robots is found as

$$\mathbf{M}_{\mathbf{x},m}\dot{\boldsymbol{\varepsilon}}_m+\alpha_{3,m}\mathbf{M}_{\mathbf{x},m}\boldsymbol{\varepsilon}_m+\mathbf{C}_{\mathbf{x},m}\boldsymbol{\varepsilon}_m=\mathbf{R}_{\mathbf{x},m}\tilde{\boldsymbol{\beta}}_{\mathbf{x},m}\tag{A5}$$

$$\mathbf{M}_{\mathbf{x},s}\dot{\boldsymbol{\varepsilon}}_s+\alpha_{3,s}\mathbf{M}_{\mathbf{x},s}\boldsymbol{\varepsilon}_s+\mathbf{C}_{\mathbf{x},s}\boldsymbol{\varepsilon}_s=\mathbf{R}_{\mathbf{x},s}\tilde{\boldsymbol{\beta}}_{\mathbf{x},s}\tag{A6}$$

REFERENCES

[1] (Who), W. H. O., 2014,
[2] Mozaffarian, D., Benjamin, E. J., Go, A. S., Arnett, D. K., Blaha, M. J., Cushman, M., De Ferranti, S., Després, J.-P., Fullerton, H. J., Howard, V. J., Huffman, M. D., Judd, S. E., Kissela, B. M., Lackland, D. T., Lichtman, J. H., Lisabeth, L. D., Liu, S., Mackey, R. H., Matchar, D. B., Mcguire, D. K., Mohler, E. R., Moy, C. S., Muntner, P., Mussolino, M. E., Nasir, K., Neumar, R. W., Nichol, G., Palaniappan, L., Pandey, D. K., Reeves, M. J., Rodriguez, C. J., Sorlie, P. D., Stein, J., Towfighi, A., Turan, T. N., Virani, S. S., Willey, J. Z., Woo, D., Yeh, R. W., and Turner, M. B., 2015, "Heart Disease and Stroke Statistics—2015 Update: A Report from the American Heart Association," Circulation, 131(4), pp. e29-e322.
[3] Blank, A. A., French, J. A., Pehlivan, A. U., and O'malley, M. K., 2014, "Current Trends in Robot-Assisted Upper-Limb Stroke Rehabilitation: Promoting Patient Engagement in Therapy," Current Physical Medicine and Rehabilitation Reports, 2(3), pp. 184-195.
[4] Krebs, H. I., and Hogan, N., 2012, "Robotic Therapy: The Tipping Point," American journal of physical medicine & rehabilitation / Association of Academic Physiatrists, 91(11 Suppl 3), pp. S290-S297.
[5] Gupta, A., and O'malley, M. K., 2006, "Design of a Haptic Arm Exoskeleton for Training and Rehabilitation," Mechatronics, IEEE/ASME Transactions on, 11(3), pp. 280-289.
[6] Hogan, N., Krebs, H. I., Sharon, A., and Charnnarong, J., 1995,
[7] Krebs, H. I., Volpe, B. T., Williams, D., Celestino, J., Charles, S. K., Lynch, D., and Hogan, N., 2007, "Robot-Aided Neurorehabilitation: A Robot for Wrist Rehabilitation," Neural Systems and Rehabilitation Engineering, IEEE Transactions on, 15(3), pp. 327-335.
[8] Riener, R., Nef, T., and Colombo, G., 2005, "Robot-Aided Neurorehabilitation of the Upper Extremities," Medical and Biological Engineering and Computing, 43(1), pp. 2-10.
[9] Gupta, A., O'malley, M. K., Patoglu, V., and Burgar, C., 2008, "Design, Control and Performance of Ricewrist: A Force Feedback Wrist Exoskeleton for Rehabilitation and Training," The International Journal of Robotics Research, 27(2), pp. 233-251.
[10] Carignan, C. R., and Krebs, H. I., 2006, "Telerehabilitation Robotics: Bright Lights, Big Future?," Journal of Rehabilitation Research and Development, 43(5), pp. 695-710.
[11] Kim, J., Kim, H., Tay, B. K., Muniyandi, M., Srinivasan, M. A., Jordan, J., Mortensen, J., Oliveira, M., and Slater, M., 2004, "Transatlantic Touch: A Study of Haptic Collaboration over Long Distance," Presence: Teleoperators and Virtual Environments, 13(3), pp. 328-337.
[12] Johnson, M., Loureiro, R. V., and Harwin, W., 2008, "Collaborative Tele-Rehabilitation and Robot-Mediated Therapy for Stroke Rehabilitation at Home or Clinic," Intelligent Service Robotics, 1(2), pp. 109-121.
[13] Reinkensmeyer, D. J., Pang, C. T., Nessler, J. A., and Painter, C. C., 2002, "Web-Based Telerehabilitation for the Upper Extremity after Stroke," Neural Systems and Rehabilitation Engineering, IEEE Transactions on, 10(2), pp. 102-108.

[14] Jadhav, C., and Krovi, V., 2004, "A Low-Cost Framework for Individualized Interactive Telerehabilitation," eds., 2, pp. 3297-3300.
[15] Tao, R., 2014, "Haptic Teleoperation Based Rehabilitation Systems for Task-Oriented Therapy," Ph.D. thesis, University of Alberta,
[16] Atashzar, S. F., Shahbazi, M., Tavakoli, M., and Patel, R. V., 2015, "A New Passivity-Based Control Technique for Safe Patient-Robot Interaction in Haptics-Enabled Rehabilitation Systems," eds., pp. 4556-4561.
[17] Shahbazi, M., Atashzar, S. F., Tavakoli, M., and Patel, R. V., 2016, "Robotics-Assisted Mirror Rehabilitation Therapy: A Therapist-in-the-Loop Assist-as-Needed Architecture," IEEE/ASME Transactions on Mechatronics, 21(4), pp. 1954-1965.
[18] Carignan, C. R., and Olsson, P. A., 2004, "Cooperative Control of Virtual Objects over the Internet Using Force-Reflecting Master Arms," eds., 2, pp. 1221-1226.
[19] Shahbazi, M., Atashzar, S. F., and Patel, R. V., 2014, "A Framework for Supervised Robotics-Assisted Mirror Rehabilitation Therapy," eds., pp. 3567-3572.
[20] Sharifi, I., Talebi, H. A., and Motaharifar, M., 2016, "A Framework for Simultaneous Training and Therapy in Multilateral Tele-Rehabilitation," Computers & Electrical Engineering, 56(pp. 700-714.
[21] Colgate, J. E., 1993, "Robust Impedance Shaping Telemanipulation," Robotics and Automation, IEEE Transactions on, 9(4), pp. 374-384.
[22] Dongjun, L., and Li, P. Y., 2003, "Passive Bilateral Feedforward Control of Linear Dynamically Similar Teleoperated Manipulators," Robotics and Automation, IEEE Transactions on, 19(3), pp. 443-456.
[23] Polushin, I. G., Liu, P. X., Lung, C.-H., and On, G. D., 2010, "Position-Error Based Schemes for Bilateral Teleoperation with Time Delay: Theory and Experiments," Journal of Dynamic Systems, Measurement, and Control, 132(3), pp. 031008 (11 pages).
[24] Chopra, N., Spong, M. W., and Lozano, R., 2008, "Synchronization of Bilateral Teleoperators with Time Delay," Automatica, 44(8), pp. 2142-2148.
[25] Nuño, E., Ortega, R., and Basañez, L., 2010, "An Adaptive Controller for Nonlinear Teleoperators," Automatica, 46(1), pp. 155-159.
[26] Liu, Y. C., and Chopra, N., 2013, "Control of Semi-Autonomous Teleoperation System with Time Delays," Automatica, 49(6), pp. 1553-1565.
[27] Liu, X., Tao, R., and Tavakoli, M., 2014, "Adaptive Control of Uncertain Nonlinear Teleoperation Systems," Mechatronics, 24(1), pp. 66-78.
[28] Ryu, J. H., and Kwon, D. S., 2001, "A Novel Adaptive Bilateral Control Scheme Using Similar Closed-Loop Dynamic Characteristics of Master/Slave Manipulators," Journal of Robotic Systems, 18(9), pp. 533-543.
[29] Liu, X., and Tavakoli, M., 2011, "Adaptive Inverse Dynamics Four-Channel Control of Uncertain Nonlinear Teleoperation Systems," Advanced Robotics, 25(13-14), pp. 1729-1750.
[30] Sharifi, M., Behzadipour, S., and Salarieh, H., 2016, "Nonlinear Bilateral Adaptive Impedance Control with Applications in Telesurgery and Telerehabilitation," Journal of Dynamic Systems, Measurement, and Control, 138(11), pp. 111010 (16 pages).
[31] Hogan, N., 1985, "Impedance Control: An Approach to Manipulation: Part I---Theory," Journal of Dynamic Systems, Measurement, and Control, 107(1), pp. 1-7.
[32] Abdossalami, A., and Sirouspour, S., 2009, "Adaptive Control for Improved Transparency in Haptic Simulations," Haptics, IEEE Transactions on, 2(1), pp. 2-14.

[33] Sharifi, M., Behzadipour, S., and Vossoughi, G., 2014, "Nonlinear Model Reference Adaptive Impedance Control for Human–Robot Interactions," Control Engineering Practice, 32(pp. 9-27.
[34] Krebs, H. I., Palazzolo, J. J., Dipietro, L., Ferraro, M., Krol, J., Rannekleiv, K., Volpe, B. T., and Hogan, N., 2003, "Rehabilitation Robotics: Performance-Based Progressive Robot-Assisted Therapy," Autonomous Robots, 15(1), pp. 7-20.
[35] Rubio, A., Avello, A., and Florez, J., 1999, "Adaptive Impedance Modification of a Master-Slave Manipulator," eds., 3, pp. 1794-1799.
[36] Dubey, R. V., Tan Fung, C., and Everett, S. E., 1997, "Variable Damping Impedance Control of a Bilateral Telerobotic System," Control Systems, IEEE, 17(1), pp. 37-45.
[37] Hashtrudi-Zaad, K., and Salcudean, S. E., 2001, "Analysis of Control Architectures for Teleoperation Systems with Impedance/Admittance Master and Slave Manipulators," The International Journal of Robotics Research, 20(6), pp. 419-445.
[38] Cho, H. C., and Park, J. H., 2005, "Stable Bilateral Teleoperation under a Time Delay Using a Robust Impedance Control," Mechatronics, 15(5), pp. 611-625.
[39] Abbott, J. J., and Okamura, A. M., 2007, "Pseudo-Admittance Bilateral Telemanipulation with Guidance Virtual Fixtures," The International Journal of Robotics Research, 26(8), pp. 865-884.
[40] Bansil, S., Prakash, N., Kaye, J., Wrigley, S., Manata, C., Stevens-Haas, C., and Kurlan, R., 2012, "Movement Disorders after Stroke in Adults: A Review," Tremor and Other Hyperkinetic Movements, 2(pp. tre-02-42-195-1.
[41] Smaga, S., 2003, "Tremor," American Family Physician, 68(8), pp. 1545-1552.
[42] Kim, J. S., 1992, "Delayed Onset Hand Tremor Caused by Cerebral Infarction," Stroke, 23(2), pp. 292-4.
[43] Slotine, J. J. E., and Li, W., 1991, *Applied Nonlinear Control*, Prantice-Hall, NJ, Englewood Cliffs.
[44] Sharifi, M., Behzadipour, S., and Vossoughi, G. R., 2014, "Model Reference Adaptive Impedance Control in Cartesian Coordinates for Physical Human–Robot Interaction," Advanced Robotics, 28(19), pp. 1277-1290.
[45] Haddadi, A., and Hashtrudi-Zaad, K., 2010, "Bounded-Impedance Absolute Stability of Bilateral Teleoperation Control Systems," Haptics, IEEE Transactions on, 3(1), pp. 15-27.
[46] Nuño, E., Basañez, L., and Ortega, R., 2011, "Passivity-Based Control for Bilateral Teleoperation: A Tutorial," Automatica, 47(3), pp. 485-495.
[47] Çavuşoğlu, M. C., Feygin, D., and Tendick, F., 2002, "A Critical Study of the Mechanical and Electrical Properties of the Phantom Haptic Interface and Improvements for High-Performance Control," Presence: Teleoperators & Virtual Environments, 11(6), pp. 555-568.
[48] Dyck, M. D., 2013, "Measuring the Dynamic Impedance of the Human Arm," Ph.D. thesis, University of Alberta,
[49] Dyck, M., and Tavakoli, M., 2013, "Measuring the Dynamic Impedance of the Human Arm without a Force Sensor," eds., pp. 1-8.

Figure Captions List

Fig. 1 The proposed resistive/assistive tele-rehabilitation strategy using an impedance-controlled tele-robotic system.

Fig. 2 The magnitude Bode diagram of an under-damped linear second order system (with natural frequency of $\omega_{n_{des}}$). The oscillatory tremor is assumed to have a minimum frequency of $\omega_{trem_{\min}}$.

Fig. 3 Block diagram of the nonlinear bilateral adaptive control of master and slave robots for resistive/assistive tele-rehabilitation.

Fig. 4 Experimental tele-robotic system for resistive/assistive tele-rehabilitation: (a) Phantom Premium robot (slave), and (b) Quanser Rehab robot (master), where healthy human operators behave as the therapist and patient.

Fig. 5 The scaled interaction forces ($\mu_f \mathbf{f}_{th}$ and $\mathbf{f}_{pa}$) in (a) x and (b) y directions for the resistive/assistive tele-rehabilitation of a patient with moderate disability and hand tremors (simulated by a healthy operator).

Fig. 6 The patient (master) and the therapist (slave) positions with the desired impedance response in (a) x and (b) y directions of resistive environment.

Fig. 7 The master and slave position tracking errors with respect to impedance responses ($\tilde{\mathbf{x}}_m$ and $\tilde{\mathbf{x}}_s$) and the slave deviation from the master position

($\mathbf{x}_s - \mu_{\mathrm{p}}\mathbf{x}_m^d$) in (a) x and (b) y directions.

Fig. 8 Trajectories of the patient, the therapist, and the desired impedance models responses in the $x-y$ plane during the resistive/assistive tele-rehabilitation.

Fig. 9 The positions of the patient's and the therapist's hands and the master and slave impedance models responses in (a) x and (b) y directions during a tele-rehabilitation task for a severely impaired patient (simulated by a healthy operator).

Fig. 10 The patient and the scaled therapist forces ($\mathbf{f}_{pa}$ and $\mu_{\mathrm{f}}\mathbf{f}_{th}$) in (a) x and (b) y directions for a severely impaired patient having considerable hand tremors (simulated by a healthy operator).

Fig. 11 The master and slave position tracking errors with respect to impedance responses ($\tilde{\mathbf{x}}_m$ and $\tilde{\mathbf{x}}_s$) and the slave deviation from the master position ($\mathbf{x}_s - \mu_{\mathrm{p}}\mathbf{x}_m^d$) in (a) x and (b) y directions.

Fig. 12 The scaled interaction forces ($\mu_{\mathrm{f}}\mathbf{f}_{th}$ and $\mathbf{f}_{pa}$), (b) the patient (master) and the therapist (slave) positions and their desired impedance responses, and (c) the master and slave position tracking errors ($\tilde{\mathbf{x}}_m$ and $\tilde{\mathbf{x}}_s$) and the slave deviation from the master position ($\mathbf{x}_{des_s} - \mu_{\mathrm{p}}\mathbf{x}_m^d$), in y direction, for a patient with moderate disability and hand tremors (simulated by a healthy operator).

Fig. 13 Trajectories of the patient, the therapist, and the desired impedance models responses in the $x-y$ plane during the resistive/assistive tele-rehabilitation.

Table Caption List

Table 1 Parameters adjustment of the first impedance model (1) for resistive/assistive tele-rehabilitation of different patients and for tremor filtration

Table 2 Parameters of the first and second desired impedance models for resistive/assistive tele-rehabilitation with different patient capabilities and communication delays $T_1 = 150\ m\text{sec}$ and $T_2 = 150\ m\text{sec}$

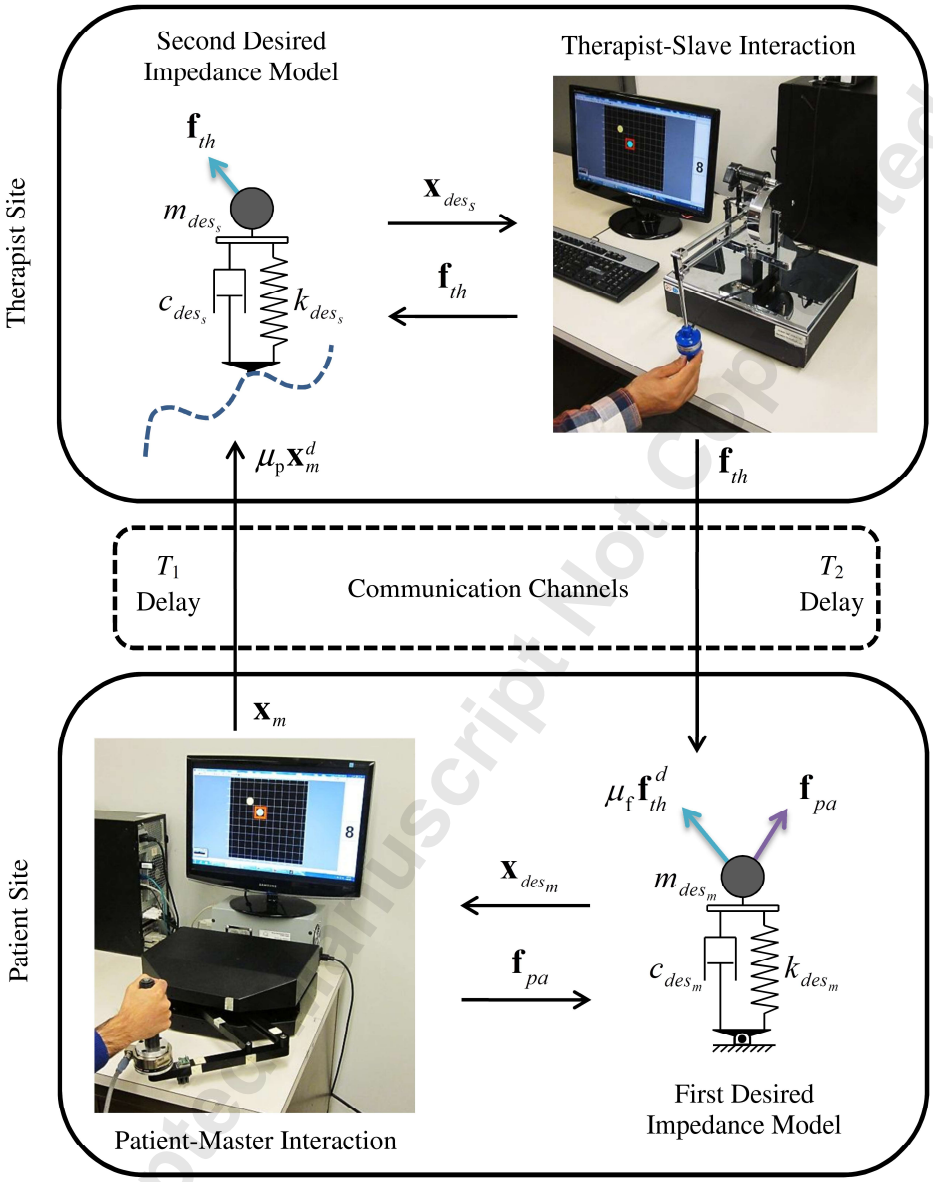

Fig. 1 The proposed resistive/assistive tele-rehabilitation strategy using an impedance-controlled tele-robotic system.

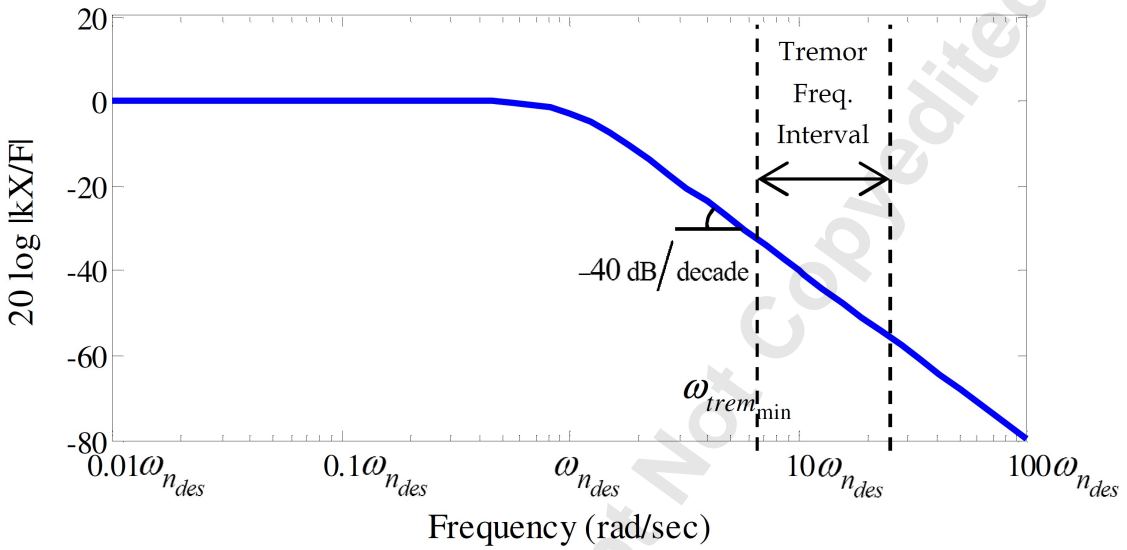

Fig. 2 The magnitude Bode diagram of an under-damped linear second order system (with natural frequency of $\omega_{n_{des}}$). The oscillatory tremor is assumed to have a minimum frequency of $\omega_{trem_{\min}}$.

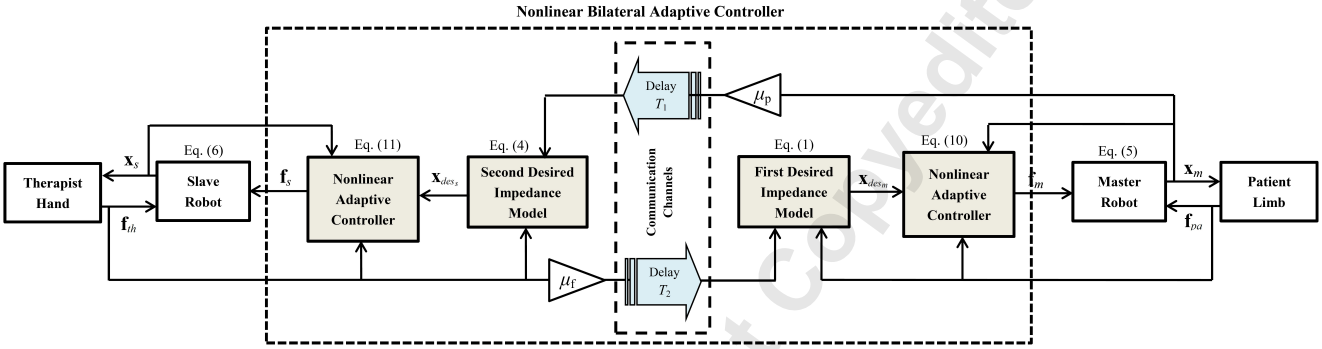

Fig. 3 Block diagram of the nonlinear bilateral adaptive control of master and slave robots for resistive/assistive tele-rehabilitation.

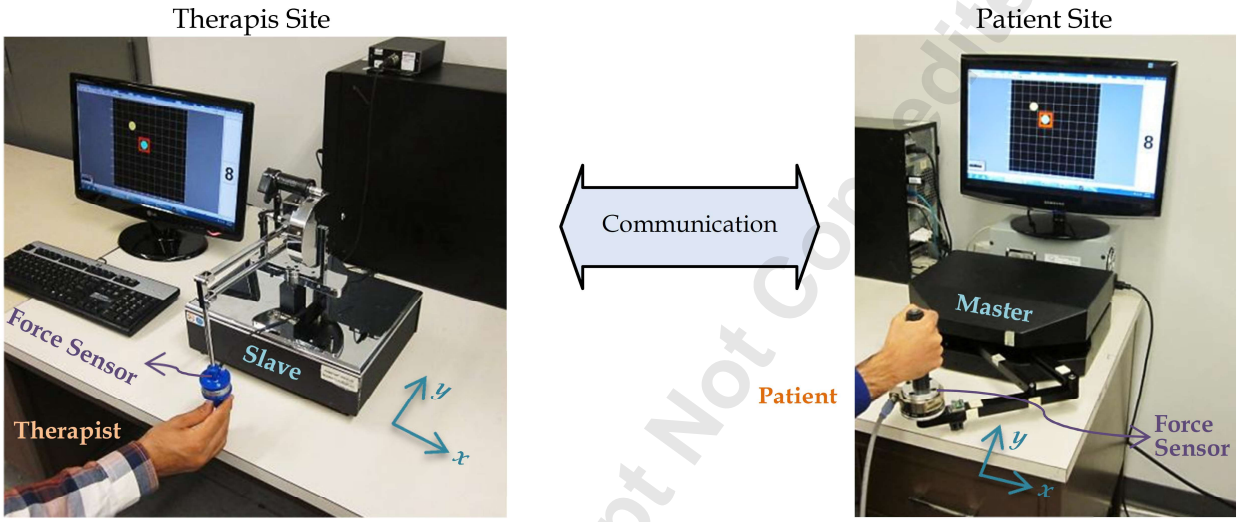

Fig. 4 Experimental tele-robotic system for resistive/assistive tele-rehabilitation: (a) Phantom Premium robot (slave), and (b) Quanser Rehab robot (master), where healthy human operators behave as the therapist and patient.

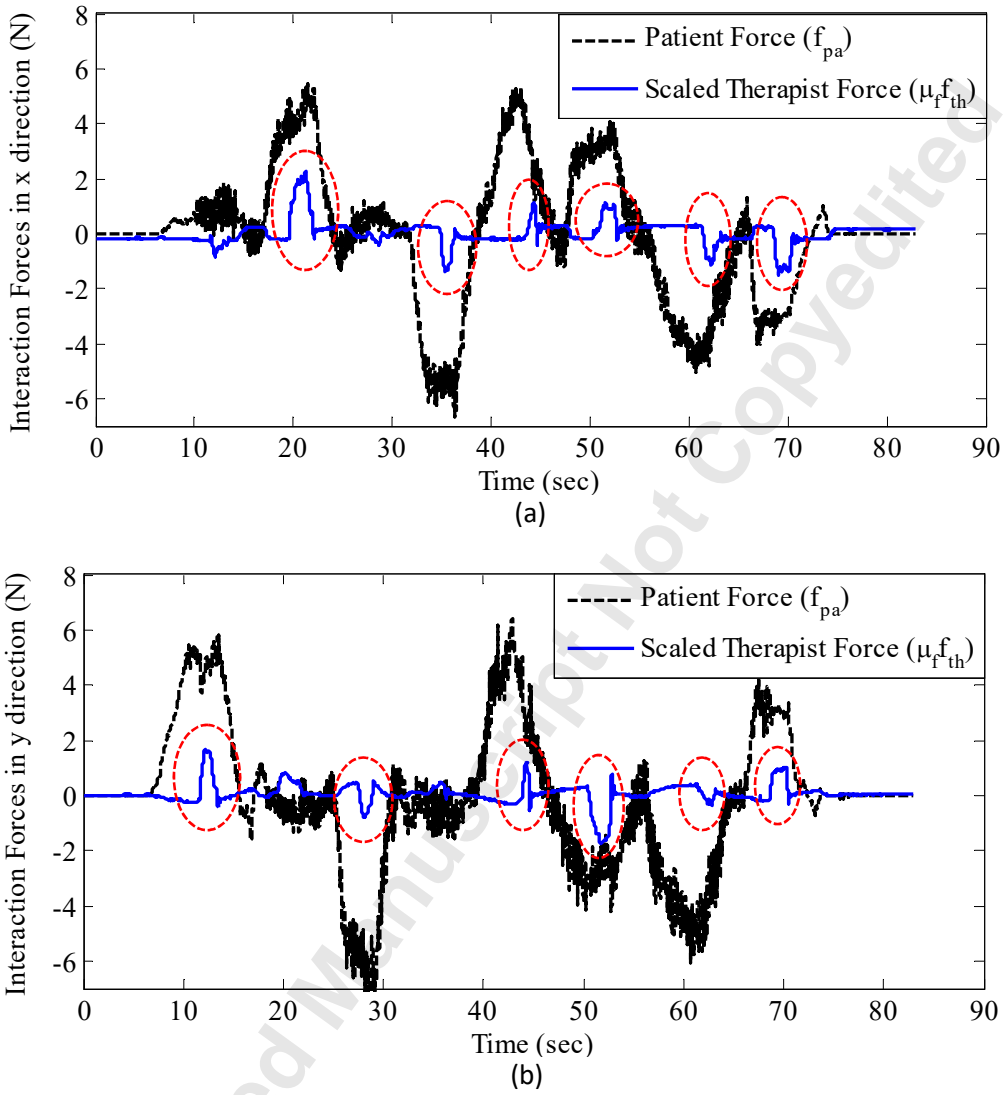

Fig. 5 The scaled interaction forces ($\mu_f \mathbf{f}_{th}$ and $\mathbf{f}_{pa}$) in (a) x and (b) y directions for the resistive/assistive tele-rehabilitation of a patient with moderate disability and hand tremors (simulated by a healthy operator).

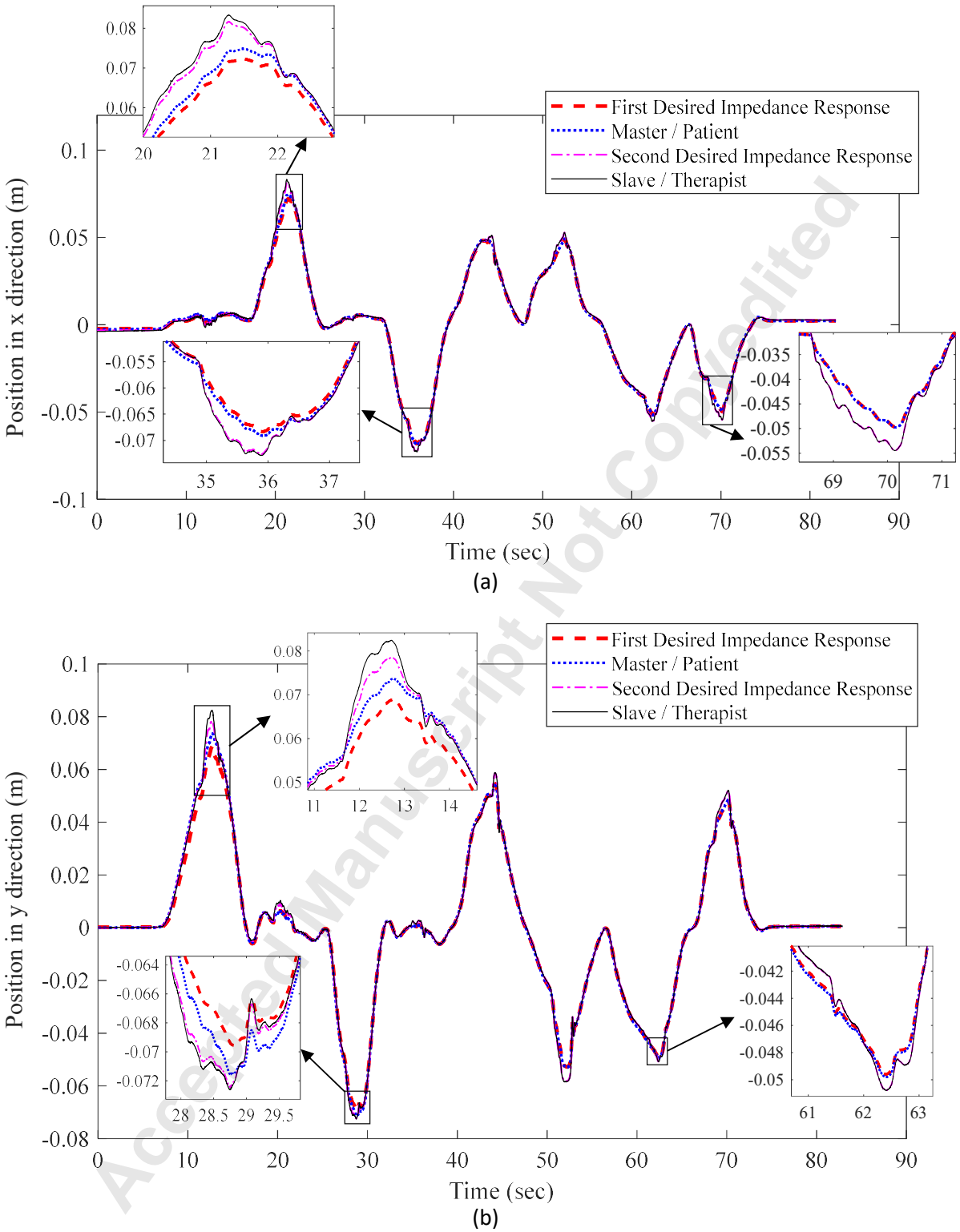

Fig. 6 The patient (master) and the therapist (slave) positions with the desired impedance response in (a) x and (b) y directions of resistive environment.

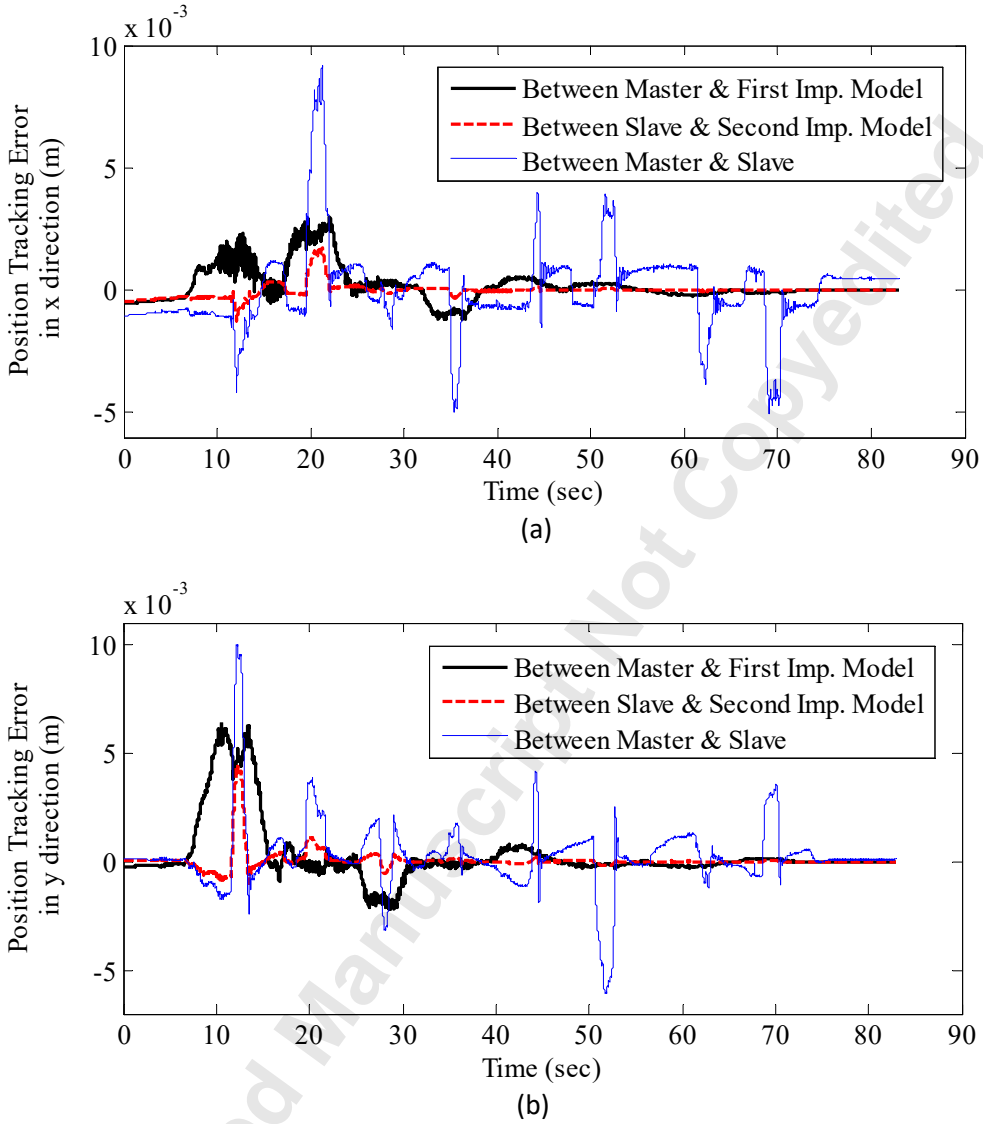

Fig. 7 The master and slave position tracking errors with respect to impedance responses ($\tilde{\mathbf{x}}_m$ and $\tilde{\mathbf{x}}_s$) and the slave deviation from the master position ($\mathbf{x}_s - \mu_{\mathrm{p}}\mathbf{x}_m^d$) in (a) x and (b) y directions.

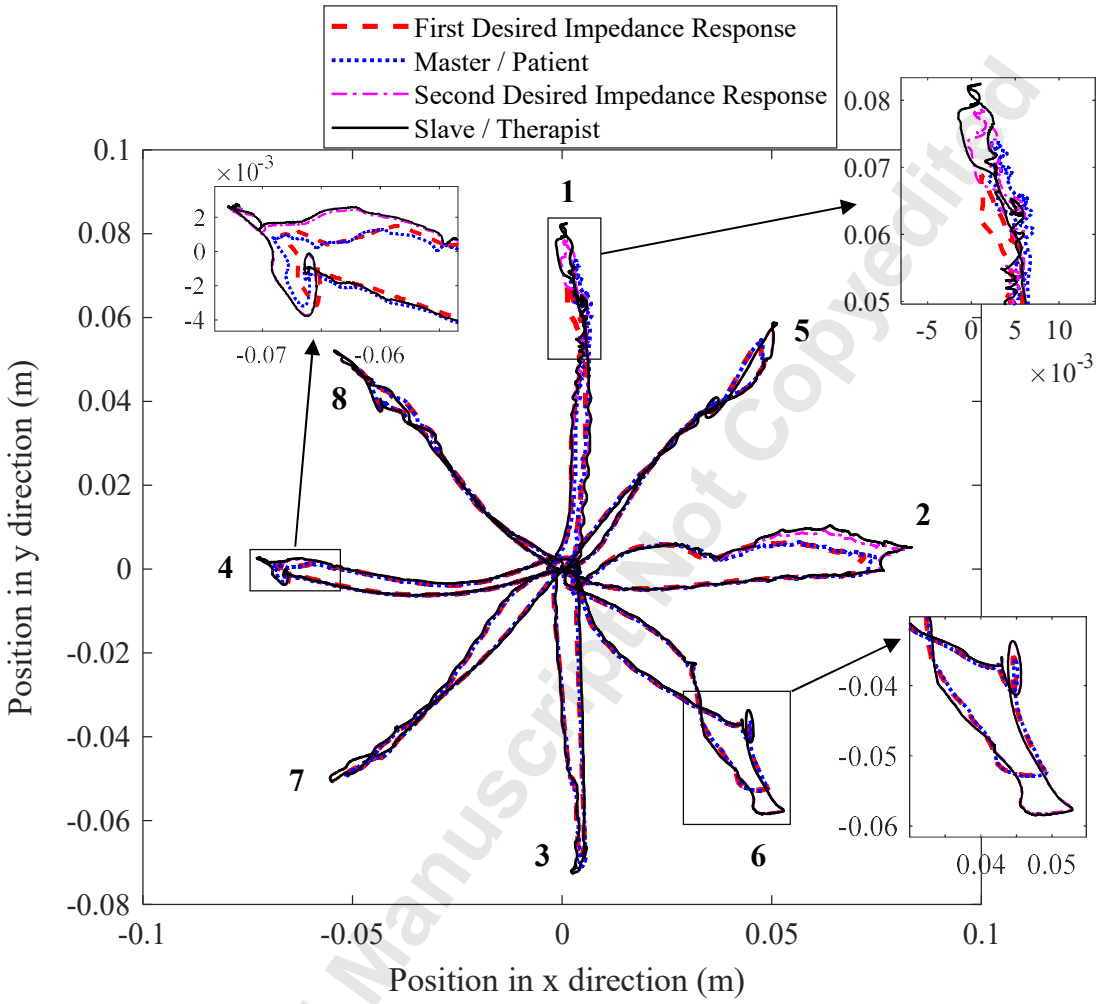

Fig. 8 Trajectories of the patient, the therapist, and the desired impedance models responses in the $x-y$ plane during the resistive/assistive tele-rehabilitation.

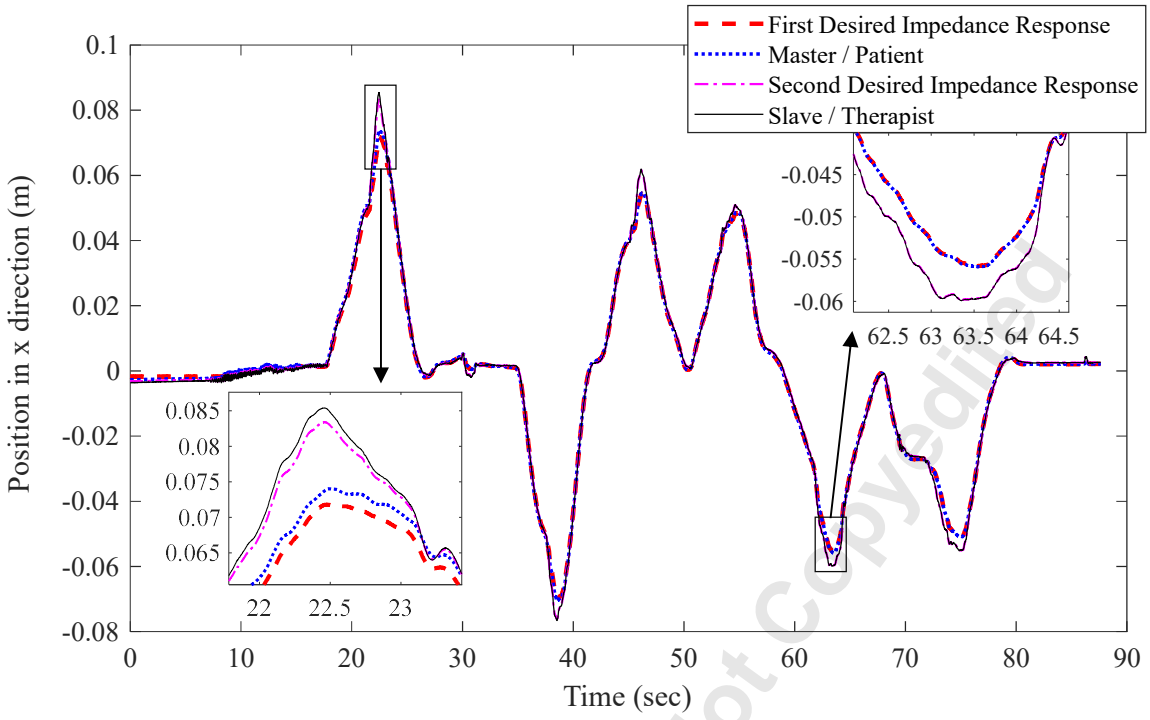

(a)

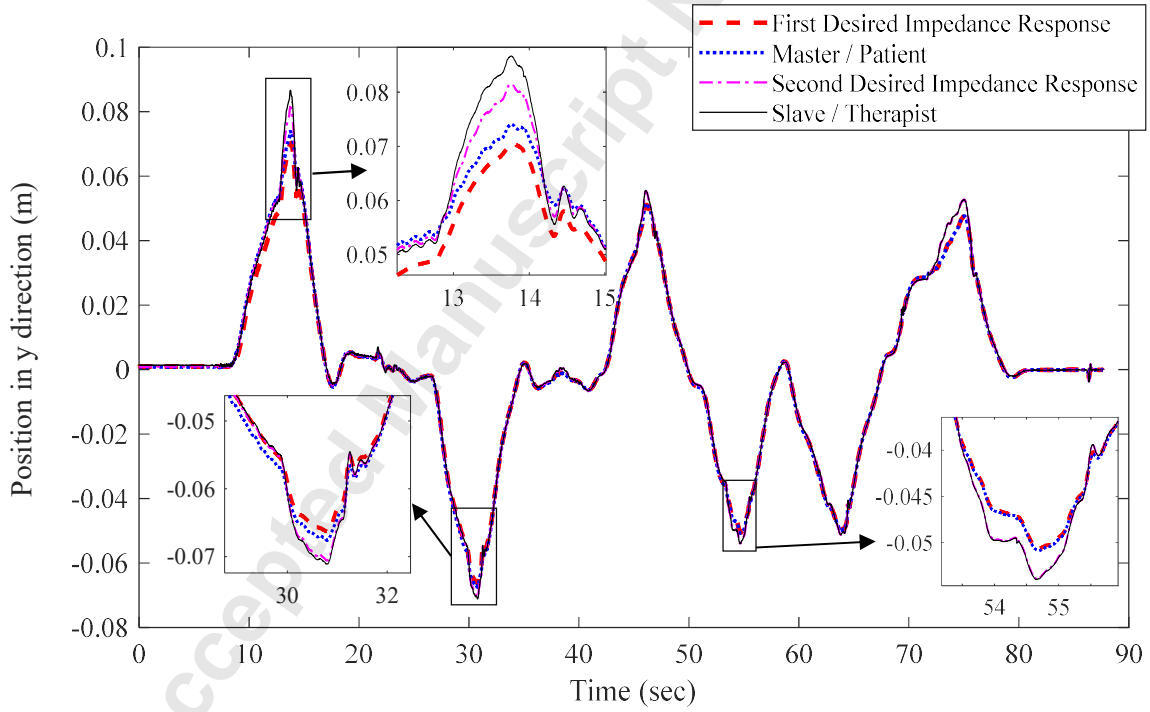

(b)

Fig. 9 The positions of the patient's and the therapist's hands and the master and slave impedance models responses in (a) x and (b) y directions during a tele-rehabilitation task for a severely impaired patient (simulated by a healthy operator).

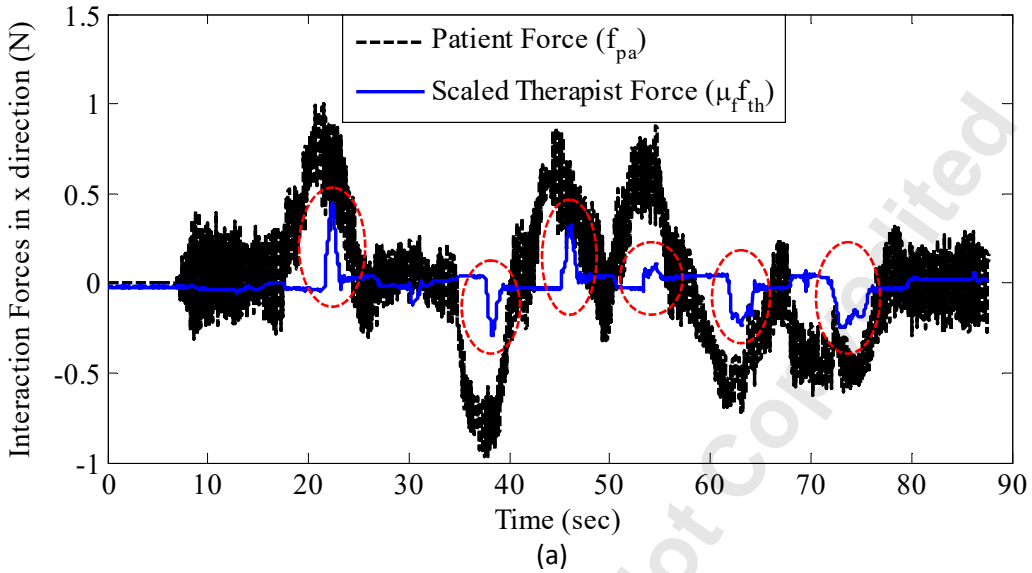

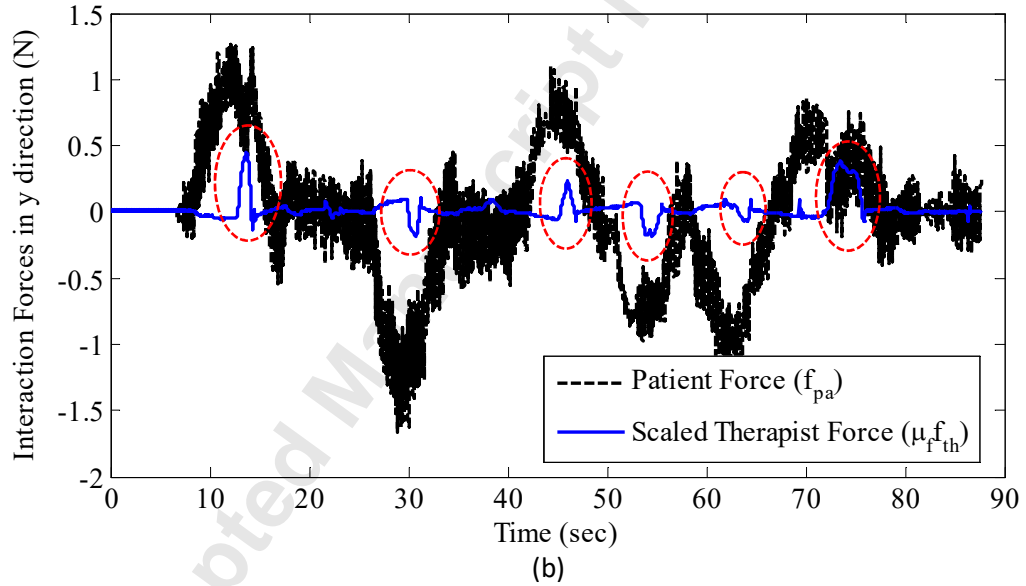

Fig. 10 The patient and the scaled therapist forces ($\mathbf{f}_{pa}$ and $\mu_f \mathbf{f}_{th}$) in (a) x and (b) y directions for a severely impaired patient having considerable hand tremors (simulated by a healthy operator).

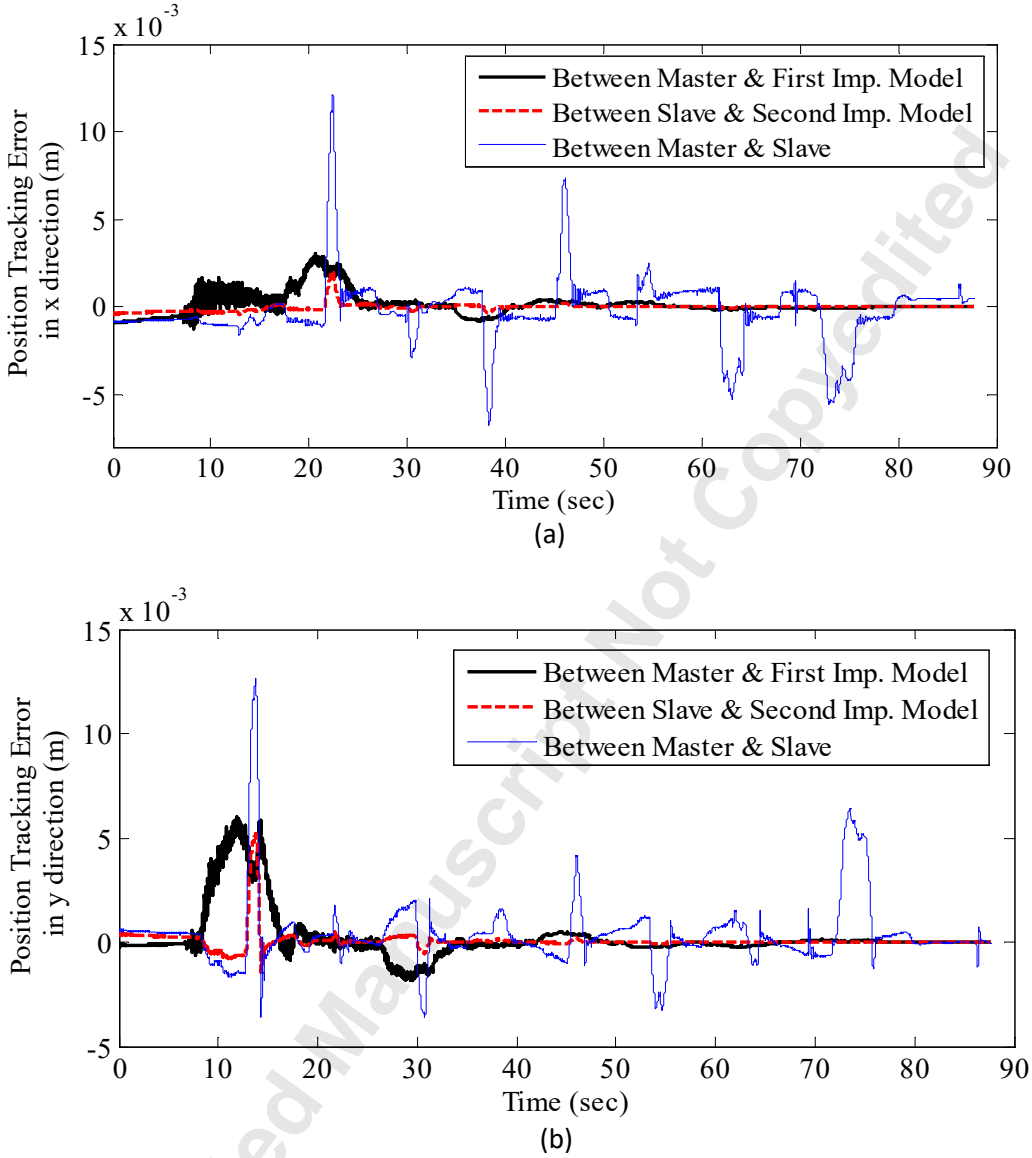

Fig. 11 The master and slave position tracking errors with respect to impedance responses ($\tilde{\mathbf{x}}_m$ and $\tilde{\mathbf{x}}_s$) and the slave deviation from the master position ($\mathbf{x}_s - \mu_{\mathrm{p}}\mathbf{x}_m^d$) in (a) x and (b) y directions.

Journal of Mechanisms and Robotics. Received July 13, 2017;
Accepted manuscript posted July 24, 2018. doi:10.1115/1.4040961

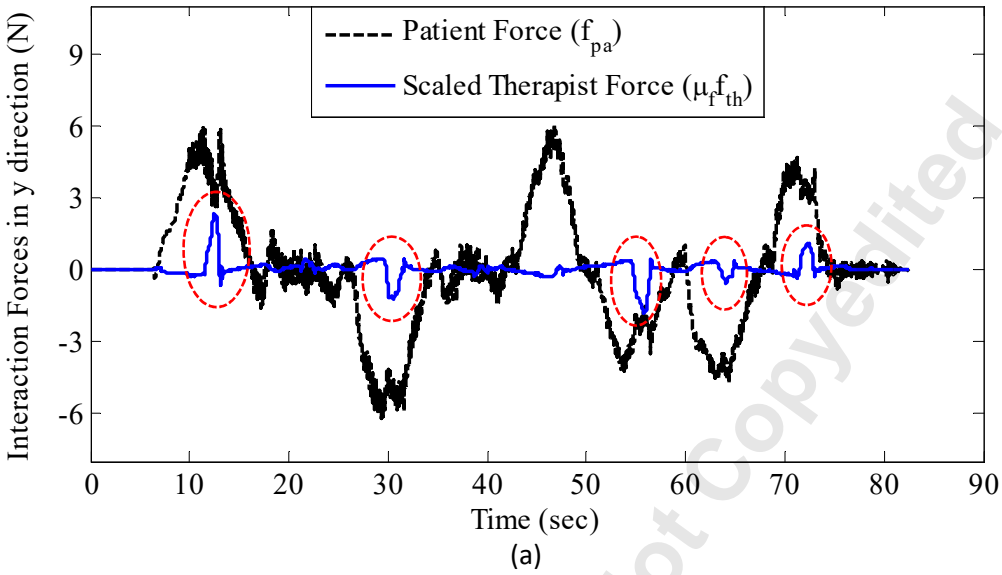

(a)

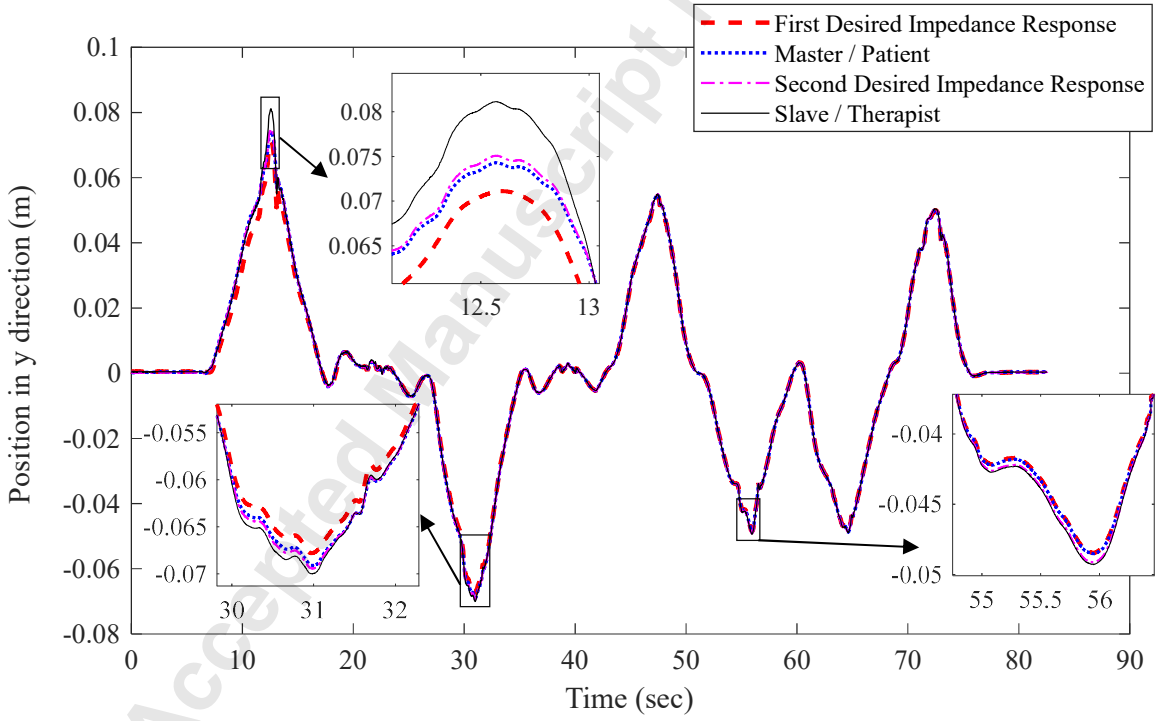

(b)

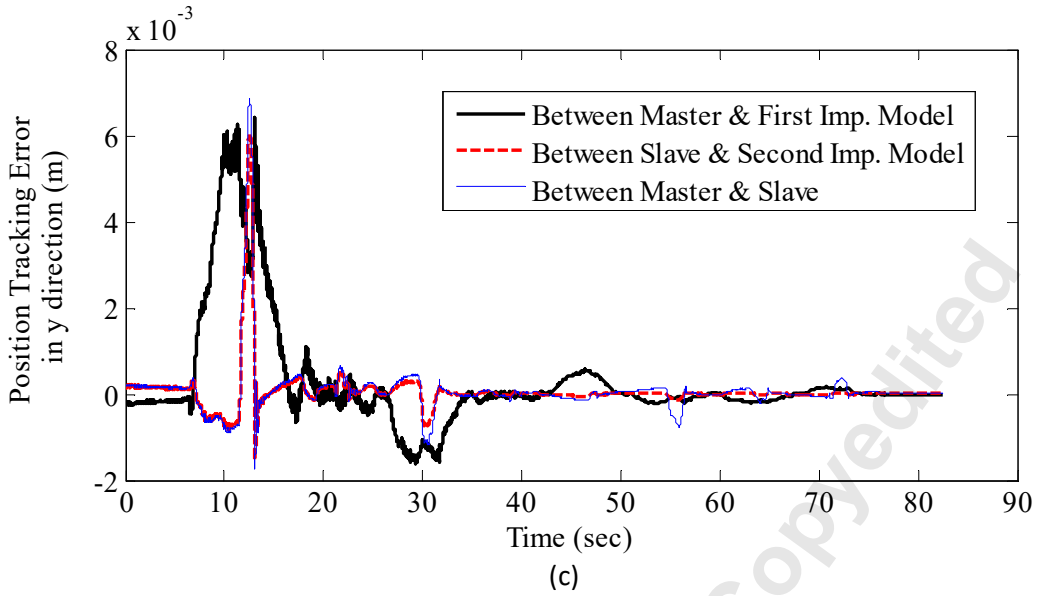

(c)

Fig. 12 (a) The scaled interaction forces ($\mu_{\mathrm{f}}\mathbf{f}_{th}$ and $\mathbf{f}_{pa}$), (b) the patient (master) and the therapist (slave) positions and their desired impedance responses, and (c) the master and slave position tracking errors ($\tilde{\mathbf{x}}_m$ and $\tilde{\mathbf{x}}_s$) and the slave deviation from the master position ($\mathbf{x}_{des_s} - \mu_{\mathrm{p}}\mathbf{x}_m^d$), in y direction, for a patient with moderate disability and hand tremors (simulated by a healthy operator).

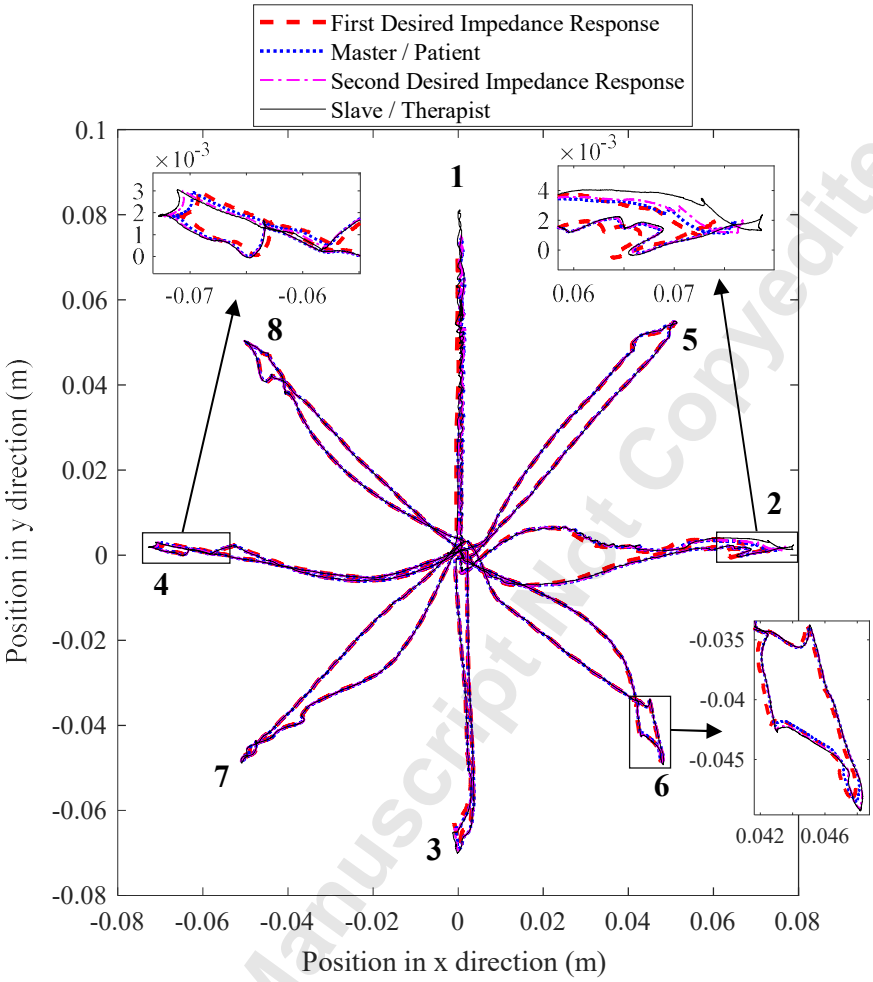

Fig. 13 Trajectories of the patient, the therapist, and the desired impedance models responses in the $x-y$ plane during the resistive/assistive tele-rehabilitation.

Table 1 Parameters adjustment of the first impedance model (1) for resistive/assistive tele-rehabilitation of different patients and for tremor filtration

	Resistive/Assistive Tele-rehabilitation		**Patient Tremor Filtration (Sec. 2.2.3)**
Application	For patients with moderate disability (Sec. 2.2.1)	For severely impaired patients (Sec. 2.2.2)	For patients with tremor
First Impedance Parameters (m_{des_m} , c_{des_m} , k_{des_m})	Moderate values	Small values	$\omega_{n_{des_m}} = \sqrt{k_{des_m} / m_{des_m}} \le 0.2\,\omega_{trem\,\min}$
Force Scaling Factor μ_{f}	Larger than 1 (e.g., $\mu_{\mathrm{f}} = 3$)	Moderate (e.g., $\mu_{\mathrm{f}} = 1$)	Due to the task

Table 2 Parameters of the first and second desired impedance models for resistive/assistive tele-rehabilitation with different patient capabilities and communication delays $T_1 = 150\ m\text{sec}$ and $T_2 = 150\ m\text{sec}$

Patient Characteristic	**First Impedance Parameters**	**Second Impedance Parameters**
With moderate disability	$k_{des_m} = 100$ N/m, $c_{des_m} = 70$ N.s/m, $m_{des_m} = 25$ kg, $\mu_f = 3$	$k_{des_s} = 100$ N/m, $c_{des_s} = 12$ N.s/m, $m_{des_s} = 0.001$ kg, $\mu_p = 1$
Severely impaired	$k_{des_m} = 20$ N/m, $c_{des_m} = 14$ N.s/m, $m_{des_m} = 5$ kg, $\mu_f = 1$	$k_{des_s} = 60$ N/m, $c_{des_s} = 8$ N.s/m, $m_{des_s} = 0.001$ kg, $\mu_p = 1$